

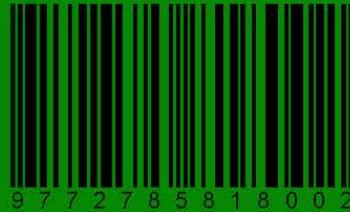


Asian Journal of Electrical and Electronic Engineering

VOLUME 4 ISSUE 1 MARCH 2024



eISSN 2785-8189



9 7 7 2 7 8 5 8 1 8 0 0 2

<https://alambiblio.com/ojs/index.php/ajoeee>



CHIEF EDITOR

Prof. Dr. AHM Zahirul Alam, IIUM, Malaysia

EXECUTIVE EDITOR

Assoc. Prof. Dr. Muhammad Mahbubur Rashid, IIUM, Malaysia

EDITORIAL BOARD MEMBERS

Prof. Dr. Sheroz Khan
Onaizah College of Engineering and Information Technology
Saudi Arab

Prof. Dr. AHM Asadul Huq
Department of Electrical and Electronic Engineering
Dhaka University, Bangladesh

Prof. Dr. Pran Kanai Shaha
Department of Electrical and Electronic Engineering
Bangladesh University of Engineering and Technology,
Bangladesh

Assoc. Prof. Dr. SMA Motakabber
Faculty of Engineering
International Islamic University Malaysia, Malaysia

Prof. Dr. ABM Harun Ur Rashid
Department of Electrical and Electronic Engineering
Bangladesh University of Engineering and Technology,
Bangladesh

Prof. Dr. Joarder Kamruzzaman
Engineering and Information Technology
Federal University, Australia

Dr. Md Arafatur Rahman
Reader in Cyber Security
University of Wolverhampton
United Kingdom

AIMS & SCOPE OF THE ASIAN JOURNAL OF ELECTRICAL AND ELECTRONIC ENGINEERING

The **Asian Journal of Electrical and Electronic Engineering (AJoEEE)**, published biannually (March and September), is a peer-reviewed open-access journal of the **Alambiblio Press**.

The Asian Journal of Electrical and Electronic Engineering publishes original research findings as regular papers and review papers (by invitation). The Journal provides a platform for Engineers, Researchers, Academicians, and Practitioners who are highly motivated to contribute to the Electrical and Electronics Engineering disciplines. It also welcomes contributions that address the developing world's specific challenges and address science and technology issues from a multidisciplinary perspective.

REFEREES' NETWORK

All papers submitted to AJoEEE Journal will be subjected to a rigorous reviewing process through a worldwide network of specialized and competent referees. Each accepted paper should have at least two positive referees' assessments.

SUBMISSION OF A MANUSCRIPT

A manuscript should be submitted online to the Asian Journal of Electrical and Electronic Engineering (AJoEEE) website <https://alambiblio.com/ojs/index.php/ajoeee>. Further correspondence on the status of the paper could be done through the journal's website



COPYRIGHT NOTICE

Consent to publish: The Author(s) agree to publish their articles with AlamBiblio Press.

Declaration: The Author(s) declare that the article has not been published before in any form. It is not concurrently submitted to another publication and does not infringe on anyone's copyright. The author (s) holds the AlamBiblio Press and Editors of the Journal harmless against all copyright claims.

Transfer of copyright: The Author(s) hereby agree to transfer the article's copyright to **AlamBiblio Press**, which shall have the non-exclusive and unlimited right to publish the article in any form, including in electronic media. For articles with more than one author, the corresponding author confirms that he/she is authorized by his/her co-author(s) to grant this transfer of copyright.

The Asian Journal of Electrical and Electronic Engineering Journal follows the open access policy.

All articles published with open access will be immediately and permanently free for everyone to read, download, copy and distribute.

ASIAN JOURNAL OF ELECTRICAL AND ELECTRONIC ENGINEERING

eISSN 2785-8189



9 7 7 2 7 8 5 8 1 8 0 0 2



Published by:

AlamBiblio Press,
PV8 platinum Hill
Jalan Melati Utama, 53100 Kuala Lumpur, Malaysia
Phone (+603) 2713 7308

Whilst the publisher and editorial board make every effort to see that no inaccurate or misleading data, opinion or statement appears in this Journal, they wish to make it clear that the data and opinions appearing in the articles and advertisements herein are the responsibility of the contributor or advertiser concerned. Accordingly, the publisher and the editorial committee accept no liability whatsoever for the consequence of any such inaccurate or misleading data, opinion or statement.



This work is licensed under a Creative Commons Attribution-Non-Commercial 4.0 International License.



Volume 4, Issue 1, March 2024

TABLE OF CONTENTS

EDITORIAL..... i

COPYRIGHT NOTICE ii

ARTICLES

IMPROVING ROTATIONAL STABILITY AND ENHANCING EFFICIENCY WITH VARIABLE INERTIAL FLYWHEELS AND MAGNETO-RHEOLOGICAL FLUIDS..... 1
Syed Munimus Salam and Muhammad Mahbubur Rashid

MODELLING AND CONTROL OF A MAGNETIC LEVITATION SYSTEM..... 9
S.M. A. Motakabber, AHM Zahirul Alam and Khairul Izham Bin Kamal

CONTROLLING THE VARIABLE INERTIA OF FLYWHEEL: A SCIENTIFIC REVIEW 17
Muhammad Mahbubur Rashid and Syed Munimus Salam

DESIGN OF A WILKINSON POWER DIVIDER WITH HARMONIC SUPPRESSION FOR MOBILE APPLICATION 29
Hanis Humaira Iskandar Tuah and AHM Zahirul Alam

Improving Rotational Stability and Enhancing Efficiency with Variable Inertial Flywheels and Magneto-Rheological Fluids

Syed Munimus Salam* and Muhammad Mahbubur Rashid

*Dept. Faculty of Mechatronics Engineering,
International Islamic University Malaysia, Kuala Lumpur, Malaysia.*

*Corresponding author: s.munimus@live.iium.edu.my

(Received:31March 2024; Accepted: 6 June 2024)

Abstract—Variations in the rotational speed of a flywheel are naturally resisted by the moment of inertia. A high moment of inertia must be maintained to minimize angular velocity variations. Conversely, a significant moment of inertia makes it difficult to start spinning machines. A flywheel with a variable moment of inertia has been suggested to solve this issue. Although fluctuations between the masses' radii across the flywheel's axis may be used to approximate true inertia, the variable inertial flywheel's (VIF) control mechanisms are somewhat complex. Magneto-rheological (MR) Fluids can be utilized to avoid the complexity of the VIF. The applied device parameters determine the design and construction of the VIF system using a relatively simple control technique. To determine the relation between the semi-active VIF control system and the input parameters of a rotating electrical machine to decrease energy losses, adequate data from a VIF coupled with an induction motor (IM) system is gathered in this study. An analysis was done on the system, and the outcome showed a possible improvement in the performance of IM. This study significantly reduces power consumption and smooth speed build-up possibility for the proposed system.

Keywords: *Variable inertia flywheel, Semi-active control, Energy Saving, Inertia Control*

1. INTRODUCTION

The flywheel is one of the most straightforward energy storage or restoration options, among many others. Because of their cheap capital costs, long cycle durability, high power density, and ability to store energy for short periods (seconds to minutes), flywheels have replaced other energy storage methods in numerous applications [1]-[4]. The primary functions of flywheels in these applications are energy storage and dampening of shaft angular velocity fluctuations. Energy storage may be used in various contexts, including flywheel hybrid vehicles, intermittent power supplies, wind turbines, and space power systems. Flywheels are often employed in AC generators, camshafts, and internal combustion engines to dampen oscillations in rotational speed [5]. The design of a flywheel with variable inertia has to be more complex than that of a flywheel with constant inertia. To have a regulated moment of inertia around its spin axis, a flywheel has to have a flexible geometry around its spin axis, and altering the geometry requires moving elements within the flywheel [6].

While the complexity of a VIF may make it heavier per unit of energy stored than a fixed inertia flywheel, the device may have a better energy density than a constant inertia flywheel if it is assumed that the VIF is replacing both the flywheel and the gearbox. Most studies in [15] focused on the design and execution of VIF in the sphere of power savings and stability. Still, they neglected to account for the effect of high system stability. There is a risk of instability and system failure due to virtual inertia control in load disturbances. This is the major drawback of the previously suggested approaches. Until now, no virtual inertia design or approach has been able to provide steady control free of device-induced fluctuations. Therefore, a robust adaptive control system must be adopted in addition to virtual inertia control to manage changes in a machine with substantial stability and energy savings.

The energy-saving potential of this flywheel has garnered a lot of interest during the last several decades. Jauch [15] suggested incorporating flywheel energy storage technology inside the rotor of a wind turbine. Figliotti and

Gomes [16] claim to have developed a vehicle-mounted flywheel with a changeable moment of inertia and a spring connection. Van de Ven [18] presented a fluidic variable inertia flywheel that can keep its angular velocity constant throughout a broad range of energy storage. The double-mass flywheel has a centrifugal pendulum similar to Ishida et al.'s [19]. James et al. [22] propose a fluidic variable inertia flywheel that can keep its angular velocity constant throughout a broad range of energy storage. According to Yuan et al. [20], a variable inertia flywheel may be used instead of a conventional fixed inertia flywheel. In this research, Bao [24] created flywheels with a movable equivalent mass moment of inertia and no permanent connection to the machine's input shaft. Matsuoka [22-23] presented new vibration suppression mechanisms using a fluid that behaved like a sequence of inertia masses. However, magnetorheological fluid has not been extensively implemented in flywheels. It has not been determined whether or not VIMRF (variable inertia magnetic rheological flywheel) can save more energy than its competitors. New approaches are emerging as research advances.

1.1 Motivation

Variable inertia to optimize the flywheel's output has been a common technique for the past few years. Many researchers addressed this issue in their research, and as a result, new techniques were introduced to control VIF. MR fluid is a recent invention used in damper control in different vibrating systems. This analysis will quantify the possibility of utilising this type of fluid to control the inertia of a VIF and will be used to improve the application system's performance.

2. PROBLEM FORMULATION AND SCOPE ANALYSIS

Whereas a variable inertial flywheel's (VIF) balancing mechanisms are relatively complex, the principle of variable inertia may be used by altering the location of the masses relative to the flywheel's axis. Furthermore, while there is abundant research on VIF control strategies, little of it concentrates on the application side. Characterizing the link between the VIF and the VIF coupled machine is crucial for reducing complexity and obtaining more effective control for the VIF that manages a broad variety of various rotating machines.

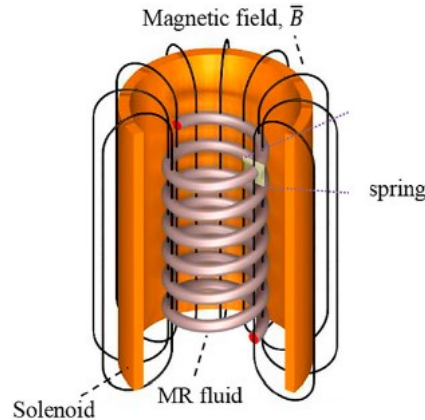


Fig. 1. Spring-solenoid system and generated magnetic field

In both the rotating flywheel and the inertia of mass, vibration is a common motion phenomenon that often oscillates around a balanced point. Because it produces obtrusive noise, uses energy, causes mechanical wear and structural stress, and raises danger, vibration in VIF is typically unwanted. Because of this, specialists have spent a lot of time researching vibration control. "Vibration control" in this context refers to lessening vibration to minimize undesirable oscillations in a protected structure. This is often achieved using a small connecting device composed of a spring, damper, or mass [14].

The primary emphasis of research over the last several decades has been on passive, active, and semi-active vibration control systems. The reaction time and operational frequency range of these systems are significantly impacted by system stiffness. Semi-active control is more stable than active control and needs less outside energy to operate as control energy. Compared to passive control, it is more versatile and works across a more extensive frequency range. As a result, semi-active control systems are pretty intriguing and are used in many different technical fields. Variables for semi-active control include damping, stiffness, or mass [15]- [16].

Non-Newtonian fluids like MR and ER transform their observable properties when subjected to magnetic or electric fields. Micron-sized iron particles suspended in a carrier fluid (water, petroleum-based oil, or silicon-based oil) change the rheological features of the fluid by aligning in chain-like patterns along the flux lines of a magnetic or electrical field. Both magnetically reversible (MR) and electrically reversible (ER) materials may undergo a phase transition from a viscous fluid to a semi-solid state when exposed to a magnetic or electric field [17].

The VIF's mechanical and control components work together to allow it to operate with MR fluid with different degrees of inertia. A mechanical system of bearings, and a spinning disc also includes a motor that can move the mass around to a new spot. Finally, an MR VIF's effectiveness is responsible for regulating the motor's speed and stability and modifying the flywheel's moment of inertia. Since dynamic adjustment permits precise control over energy storage and discharge, understanding MR VIF's performance analysis is essential.

3. VIF APPLICATION AND TECHNIQUE

In a flywheel with variable inertia, the slider's passage through the slot causes the flywheel's inertia to change. Fig. 3 depicts the conceptual design of the VIF. As the flywheel speed counted zero, the inserted springs are at free length initially and contact the hub. Here, gravity's impact is disregarded. The springs can only be compressed; they cannot expand farther. [18].

An engineered container has been used to demonstrate the concept of a flywheel with a variable moment of inertia; as the liquid inside the container spreads out at higher velocities, the container's moment of inertia shifts from that of a disk-type flywheel to that of a hoop-type flywheel, despite their shared mass and outer radius. Even though the quantity of energy extracted within the defined speed range is comparable to that of a flywheel with a hoop-like construction, the percentage of extractability increases by more than 10%. Moreover, below the lower speed limit, wasted energy is reduced by 50%. There are several restrictions to the demonstration flywheel, but a design method and many potential parameters have been offered in Design of a Liquid-Based Variable Inertia Flywheel by J. Barid (2014) [19]. To combine the issues, the MR VIF is constructed to remotely control the mass and reduce vibration sufficiently.

The moment of inertia of the slider about its own mass center and that of the fixed structural part about the shaft center, respectively, are expressed as

$$J_s = \frac{1}{4} M_s \left(\frac{d_s^2}{4} + \frac{I_s^2}{3} \right) \dots \dots \dots (1)$$

$$J_F = J_{shaft} + J_{scd} - N J_{slot} \dots \dots \dots (2)$$

where,

$J_{scd} = \frac{1}{4} M_{scd} (r_s^2 + r_0^2)$ is the polar moment of inertia of a solid flywheel of uniform thickness

J_{shaft} is the polar moment of inertia of the shaft

$$J_{slot} = m_{slot} \left\{ \frac{1}{12} (d_s^2 + I_{slot}^2) + (r_0 + .5 I_{slot})^2 \dots \dots \dots (3) \right. [18]$$

A spring is inserted between the frame and the piston. The coil set to excite the fluid is inserted in the middle of the double-ring groove surrounded by the piston.

If we consider friction force F_f , the spring force F_0 , MR damping force F_{mrf} , $\sin w$ is a sign function related to the radial slip velocity of piston and k is the spring constant

$$J_{slot} = m_{slot} \left\{ F_0 + (F_{mrf} + F_f) \sin w + k \frac{r_i}{m_{slot} \omega^2 - k} \dots \dots \dots (4) \right. [20]$$

A fluid was used to operate as a succession of inertia masses in S M Salam [21] and L. Islam's [22] proposal for a novel vibration suppression system that uses changeable inertia mass.



Fig. 2. VIF with MR Fluid

3.1 Inertia Controlling with Smart Material

A magnetic field may be used to regulate the viscosity of a family of intelligent materials known as magnetorheological (MR) materials [23]. They are made up of magnetically sensitive, non-colloidal particles, often iron or iron-carbide, suspended in a magnetically inert matrix material. A magnetic field causes the magnetic particles to form chain-like formations, raising the matrix's effective viscosity.

Magneto-rheological fluid (MRF) is the term used to describe the resulting combination most often [24]. A fluid. Elastomers may also be employed as the matrix material because of their increased viscosity when there is no magnetic field [25]. There are also magnetorheological foams, in which a spongy substance, such as a metal foam, is soaked in an MRF or MR elastomer. [26]. The magnetic particles, base fluids, and additives are the three primary elements of MRF [27]. The magnetically active component consists of magnetic particles that, when exposed to a magnetic field, produce patterns resembling chains. The base fluid serves as a carrier and lubricant and also offers traditional damping.

Numerous qualities, including friction, corrosion, sedimentation, and viscosity, are improved by using additives. The behavior of the fluid in both its off-state and on-state is impacted by all three of these elements [28].

4. EXPERIMENTAL SETUP AND DATA COLLECTION

In this research, we used semi-active material MRF 140 CG, which has a viscosity between 0.31 to 0.27 Pas at 30° C, and for MR properties, an externally induced magnetic field is used to excite the fluid. Initially, an experimental setup was developed for data collection. A single induction motor applies and operates the flywheel system. A multimeter has measured the electrical system's parameters, and a converter regulates the system's speed. In order to alter velocity, the converter modifies both current and voltage.

The flywheel is initially put through its paces using a fixed load to ensure stability and eliminate undesirable vibrations. In the second scenario, a spring is installed to avoid the mass's damping force and prevent unwanted vibration. Power use data is kept for different speeds to be compared afterwards. At long last, MR fluid has been introduced to the system. Here, Variable Inertia cylinders filled with MR fluid are subjected to an external magnetic field to measure the resulting change in viscosity, and the resulting variations in power consumption at different speeds are recorded.

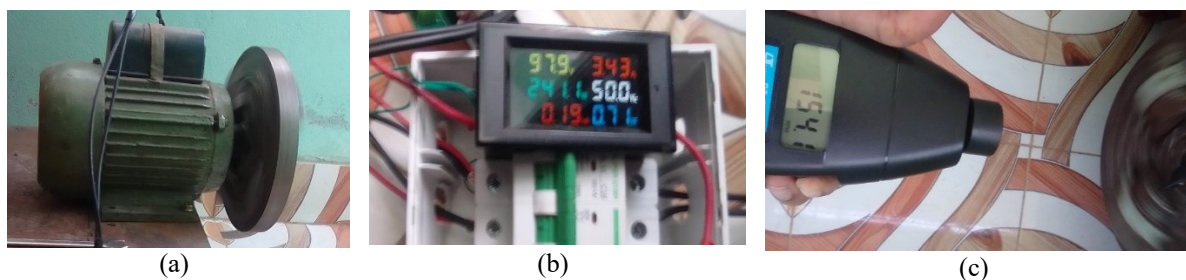


Fig. 3. Experimental Data collection (a) moving flywheel (b) electrical parameter measurement (c) speed measurement

4.1 Case Study 1: VIF with Spring Setup

Initial measurements have been made using a VIF with a spring configuration and a fixed voltage. Figure 5 (a) depicts the granular data for the 500 RPM speed, showing that power usage rises at startup but stabilizes shortly afterwards. The rate of current consumption changed throughout time. In this case, the current consumption is close to 6.8 to 7 amperes.

Figure 5 (b) compares the power usage at 700, 900, and 1100 RPM. As is the norm, initial power usage is more significant than average but drops down with time. Case Study 1's overall performance analysis results are reported in Table 1. High consumption values are proportional to increases in speed, whereas low speeds result in lower average consumption.

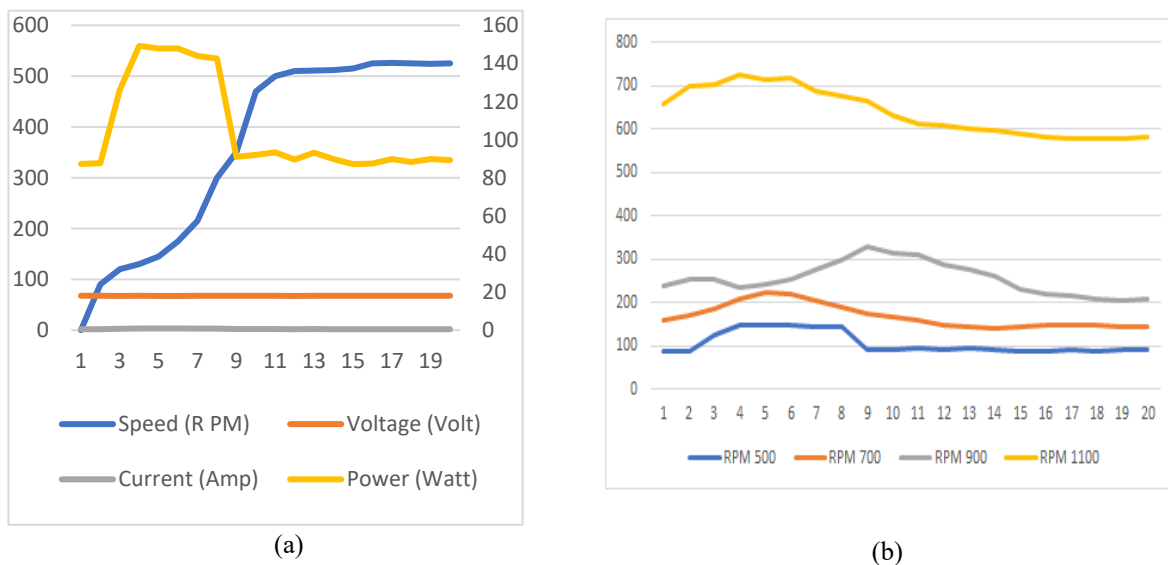


Fig.4. Power consumption analogy with speed increment for different speeds with spring set up.

Table1: Analysis of different parameters of Case 1

Speed (RPM)	Consumption (W)			Stable Time (S)	
	High	Average	Low	Speed	Consumption
500	149.18	105.64	87.2	12	9
700	221.2	167.85	142.8	10	12
900	328.6	255.58	204.5	9	15
1100	689.8	638.84	576.2	6	11

Higher speed levels take less time to stabilize than lower ones. In contrast to the features of motion, the stabilization of power consumption exhibits an inverse tendency.

4.2 Case Study 2: VIF with MRF

In the second case study, the system was operated using MR fluid within the variable inertia cylinder. Power consumption, speed stabilization, and viscosity increase while the system operates in a magnetic environment. The viscosity of the MR fluid is measured to be 0.29 Pas, and the motor is driven at several speeds. Figure 5 displays the overall performance curve in relation to the spring configuration and Figure 6 shows the Comparative study of speed build-up for 900 RPM speed.

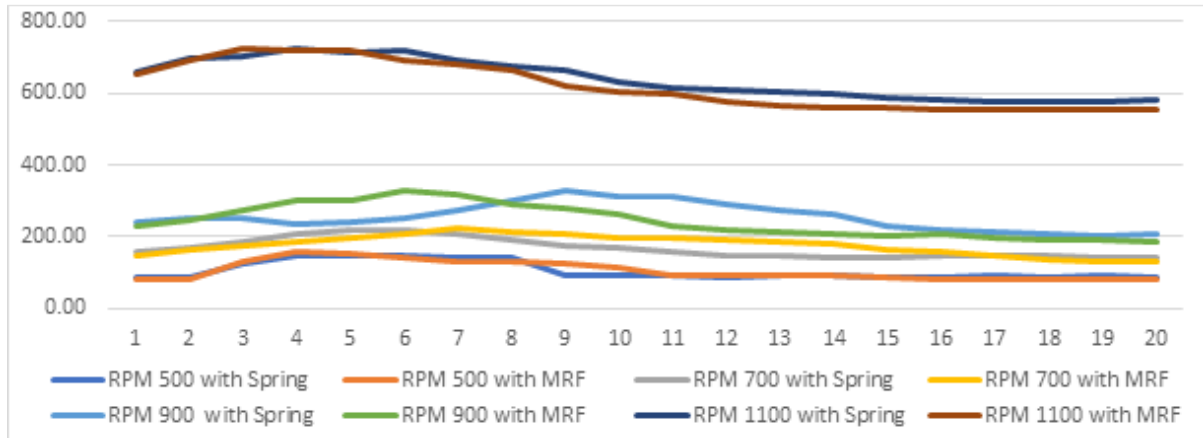


Fig. 5. Comparative study of power consumption with different speed

Table2: Analysis of different parameters of Case 1 and Case 2

Speed RPM *100	Consumption Spring (W)			Consumption MRF (W)		
	H	Avr	L	H	Av	L
5	149.1	105.64	87.2	155.7	105.4	81.1
7	221.2	167.85	142.8	222.1	165.1	133.2
9	328.6	255.58	204.5	329.3	243.2	187.7
11	689.8	638.84	576.2	726.1	619.3	554.7



Fig. 6. Comparative study of speed build-up for 900 RPM speed

4.3 Discussion

When MR fluid is used, the overall power consumption drops, but the peak value is still more significant than it would be with a spring configuration, as shown in the comparison between cases 1 and 2. When comparing the two scenarios regarding speed, the second one has a more consistent velocity than the first. That issue can define the main reason for lower power consumption with MR fluid.

5. CONCLUSION

According to inertia control theory, the semi-active Controller might be used when traditional vibration control is ineffective. Two of the most obvious would be the car and civil construction sectors, both of which are heavily reliant on controllers in the present day. However, the application side was considered by power consumption fluctuation in this analysis. Therefore, any loaded induction motor's energy consumption may be recycled if the

MRF uses vibration absorbers for VIF. Finally, it seems this sector has great potential for shedding light on the practicality of energy-saving vibration control systems.

REFERENCES

- [1] O. Farhadi, M., Mohammed, "Energy storage technologies for high power applications," IEEE Trans. Ind. Appl, vol. 52, no. 3, pp. 1953–1961, 2016.
- [2] A. Lazarewicz, M.L., Rojas, "Grid frequency regulation by recycling electrical energy in flywheels," Power Eng. Soc. Gen. Meet., vol. 2, pp. 2038–2042, 2004.
- [3] J. A. Kirk, "Flywheel energy storage—I," Int. J. Mech. Sci., vol. 19, no. 4, pp. 223–231, Jan. 1977, doi: 10.1016/0020-7403(77)90064-9.
- [4] V. Kartašovas, V. Barzdaitis, and P. Mažeika, "Modeling and simulation of variable inertia rotor," J. Vibroengineering, vol. 14, no. 4, pp. 1745–1750, 2012.
- [5] G. Zhong, Q.C.;Weiss, "Synchroverter: Inverters that mimic synchronous generators," IEEE Trans. Ind. Electron, vol. 58, pp. 1259–1265, 2011.
- [6] C. Jauch, "Controls of a Flywheel in a Wind Turbine Rotor," Wind Eng. 2016, vol. 40, pp. 173–185.
- [7] Figliotti MP and Gomes MW, "A variable-inertia flywheel model for regenerative braking on a bicycle," ASME 2014 Dyn. Syst. Control Conf. San Antonio, New York Am. Soc. Mech. Eng.
- [8] V. de V. J. Fluidic, "variable inertia flywheel.," 7th Int. energy Convers. Eng. Conf. Denver, CO, 2–5 August 2009, Pap. no. AIAA2009- 4501. Reston, VA Am. Inst. Aeronaut. Astronaut.
- [9] U. M. Ishida Y I T, Fukami T, "Torsional vibration suppression by roller type centrifugal vibration absorbers," J. Vib. Acoust. 131, pp. 1–10, 2009.
- [10] J. V. D. V, "Fluidic variable inertia flywheel and flywheel accumulator system," 2012.
- [11] Z. F. M. and X. G. X. Yuan L G, "Research on the design and control strategy of variable inertia flywheel in diesel generator unit under pulsed load," Int. Conf. Comput. Control Ind. Eng. 187-9, 2010.
- [12] H. H. Y. and L. D. Y. Bao E, "The theory and synthesis of high effect flywheel with variable equivalent mass moment of inertia," Adv. Mater. Res. 199-200 225-31, 2011.
- [13] M. T, "Vibration suppression device having variable inertia mass by MR-fluid," ASME 2011 Int. Des. Eng. Tech. Conf. Comput. Inf. Eng. Conf. 1181-5, 2011.
- [14] D. J. Inman, Engineering Vibration, Internatio. Prentice-Hall International, Inc, 1994.
- [15] Y. Liu, "Semi-active damping control for vibration isolation of base disturbances," Diss. Univ. Southampt., 2004.
- [16] M. Trikande, N. Karve, R. Anand Raj, V. Jagirdar, and R. Vasudevan, "Semi-active vibration control of an 8x8 armored wheeled platform," J. Vib. Control, vol. 24, no. 2, pp. 283–302, Jan. 2018, doi: 10.1177/1077546316638199.
- [17] N. Eslaminasab, "Development of a Semi-active Intelligent Suspension System for Heavy Vehicles," p. 181, 2008.
- [18] A. C. Mahato, S. K. Ghoshal, and A. K. Samantaray, "Influence of variable inertia flywheel and soft switching on a power hydraulic system," SN Appl. Sci., vol. 1, no. 6, p. 605, Jun. 2019, doi: 10.1007/s42452-019-0623-0.
- [19] J. Braid, "Conceptual design of a liquid-based variable inertia flywheel for microgrid applications," ENERGYCON 2014 - IEEE Int. Energy Conf., no. 2, pp. 1291–1296, 2014, doi: 10.1109/ENERGYCON.2014.6850589.
- [20] X. Dong, J. Xi, P. Chen, and W. Li, "Magneto-rheological variable inertia flywheel," Smart Mater. Struct., vol. 27, no. 11, p. 115015, Nov. 2018, doi: 10.1088/1361-665X/aad42b.

-
- [21] S. M. Salam and M. M. Rashid, "A new approach to analysis and simulation of flywheel energy storage system," in 8th International Conference on Mechatronics Engineering (ICOM 2022), 2022, pp. 90–94, doi: 10.1049/icp.2022.2271.
- [22] L. Islam, M. M. Rashid, and M. A. Faysal, "Investigation of the Energy Saving Capability of a Variable Inertia Magneto-Rheological (MR) Flywheel," vol. 2, no. 1, pp. 25–31, 2022.
- [23] J. D. Carlson and M. R. Jolly, "MR fluid, foam and elastomer devices," *Mechatronics*, vol. 10, no. 4, pp. 555–569, 2000, doi: 10.1016/S0957-4158(99)00064-1.
- [24] M. J. Wilson, A. Fuchs, and F. Gordaninejad, "Development and characterization of magnetorheological polymer gels," *J. Appl. Polym. Sci.*, vol. 84, no. 14, pp. 2733–2742, 2002, doi: 10.1002/app.10525.
- [25] X. H. Liu, P. L. Wong, W. Wang, and W. A. Bullough, "Feasibility study on the storage of magnetorheological fluid using metal foams," *J. Intell. Mater. Syst. Struct.*, vol. 21, no. 12, pp. 1193–1200, 2010, doi: 10.1177/1045389X10382585.
- [26] E. J. R. Hardy, "The magnetic fluid clutch," *Students Q. J.*, vol. 22, no. 86, p. 51, 1951, doi: 10.1049/sqj.1951.0064.
- [27] W. Lu, Y. Luo, L. L. Kang, and D. Wei, "Characteristics of magnetorheological fluids under new formulation," *J. Test. Eval.*, vol. 47, no. 4, 2019, doi: 10.1520/JTE20170477.
- [28] A. G. Olabi and A. Grunwald, "Design and application of magneto-rheological fluid," *Mater. Des.*, vol. 28, no. 10, pp. 2658–2664, 2007, doi: 10.1016/j.matdes.2006.10.009.
-

Modelling and Control of a Magnetic Levitation System

S. M. A. Motakabber*, AHM Zahirul Alam and Khairul Izham Bin Kamal

*Dept. of Electrical and Computer Engineering,
International Islamic University Malaysia, Kuala Lumpur, Malaysia*

*Corresponding author: amotakabber@iium.edu.my

(Received: 31 March 2024; Accepted: 6 June 2024)

Abstract— Magnetic Levitation Systems (MLS), or Maglev for short, utilise magnetic fields to levitate objects. They find applications in various scientific fields, particularly transportation, materials science, and biomedical engineering. Due to the diverse applications, different modelling and control approaches are necessary. The operation of each Maglev system depends on specific physical parameters. These key variables include the weight of the object being levitated, the current supplied to the system, the internal resistance and inductance of the electromagnet, and the distance between the object and the electromagnet. This research aims to understand the working principles of MLS. We will design and simulate a model based on real MLS hardware using MATLAB & Simulink. Additionally, we will create a functional Maglev prototype and program its control system using Arduino IDE and an Arduino microcontroller. MATLAB & Simulink offer a powerful tool for creating behavioral models for MLS. This model will then be integrated with Arduino programming to control the Maglev prototype.

Keywords: Magnetic Levitation System, Modelling and Control, PID, Arduino IDE

1. INTRODUCTION

The Maglev system, or MLS, is an electromechanical system that allows an object to be suspended in free space without any physical support. [1]. Magnetic levitation is a well-known type of system with numerous uses. Magnetic suspension technology is becoming increasingly popular because of its contactless, low-noise, and low-friction properties. [2]. Modelling the Maglev system is difficult since An open-loop unstable system with quick dynamics needs to be dealt with in addition to nonlinearities and a low natural damping degree. [3].

MLS comprises a suspended object or plant, a position sensor, an actuator, a power amplifier, a controller, and other components [1] Wrapping an electrically conductive wire around a high-permeability iron core forms an electromagnet. The actuator produces a magnetic field when an electrical current is delivered through the wires.

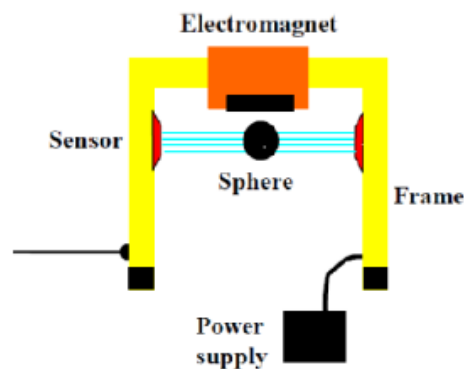


Fig. 1: Magnetic Levitation System [4]

Any magnetic item put underneath this magnetic field experiences an upward attracting force. The suspended object is placed between the electromagnet and the sensor beneath the ferromagnetic ball. The ferromagnetic ball is moved by two forces: the gravity field and the electromagnetic force “Fem” produced by the magnetic field of the coil. [4].

2. METHODOLOGY

2.1 Modelling of the Magnetic Levitation System

In electromechanical dynamics modelling, Kirchhoff's voltage law can be used to achieve the electromagnetic force produced by a current within the coil. [5].

$$V(t) = V_R + V_L = R_i + \frac{d[L(x)i]}{dt} \quad (1)$$

V is the applied input voltage, i is the current in the coil, and R is the coil's resistance [5].

Newton's third Law of motion while ignoring the damping force & friction force of air, the total force acting on the coil is given as;

$$CapF_{acc} = F_{gravity} - F_{em} \quad (2)$$

$$m\ddot{x} = mg - k \frac{i^2}{x^2} \quad (3)$$

Mathematical modelling combines both mechanical and electromagnetic dynamic modelling. It is possible to define MLS in terms of the Equation below for this model, which is explained in [6].

$$\frac{dx}{dt} = v \quad (4)$$

$$e = R_i + \frac{d[L(x)i]}{dt} \quad (5)$$

$$m \frac{d^2x}{dt^2} = mg - c \frac{i^2}{x^2} \quad (6)$$

$$u = iR + L \frac{di}{dt} - c \left(\frac{1}{x}\right)^2 \frac{dx}{dt} \quad (7)$$

Where v is the suspended ball's velocity, x is its position, m is its mass, c is the magnetic force constant, g is the gravitational constant, L and R are the coil's inductance and resistance, i is the current in the electromagnetic coil, and u is the system's applied voltage [6].

Taking $x = x_1$, $v = x_2$ and $I = x_3$ from the Equation above, the vector form of the mathematical model can be defined as:

$$\begin{bmatrix} \dot{x}_1 \\ \dot{x}_2 \\ \dot{x}_3 \end{bmatrix} = \begin{bmatrix} x_2 \\ g - \frac{c}{m} \left\{ \frac{x_3}{x_1} \right\}^2 \\ -\frac{R}{L} x_3 + \frac{2c}{L} \left\{ \frac{x_2 x_3}{x_1^2} \right\} \end{bmatrix} + \begin{bmatrix} 0 \\ 0 \\ \frac{1}{L} \end{bmatrix} \quad (8)$$

$$y = [x_1 \ x_2 \ x_3]^T = [1 \ 0 \ 0] \quad (9)$$

$$\dot{x} = f(x) + g(x)u \quad (10)$$

At equilibrium, the rate of x with respect to time must be equal to zero ($\dot{x}_{02} = 0$), and the equilibrium current must satisfy the following condition:

$$x_{03} = x_{01} \sqrt{\frac{gm}{c}} \quad (11)$$

Using all equations from above can form a linearized model, given as this state-space modelling;

$$A = \begin{bmatrix} 0 & 1 & 0 \\ Cx_{03}^2 & 0 & -2\frac{Cx_{03}}{mx_{01}^2} \\ 0 & 2\frac{Cx_{03}}{Lx_{01}^2} & -\frac{R}{L} \end{bmatrix}; B = \begin{bmatrix} 0 \\ 0 \\ \frac{1}{L} \end{bmatrix}; C = [1 \ 0 \ 0]; D = [0] \quad (12)$$

Replacing the values with the Equation above will give:

$$A = \begin{bmatrix} 0 & 1 & 0 \\ \frac{g}{x_{01}} & 0 & -\frac{2}{x_{01}} \sqrt{\frac{gc}{m}} \\ 0 & \frac{2}{L} \sqrt{gmc} & -\frac{R}{L} \end{bmatrix}; B = \begin{bmatrix} 0 \\ 0 \\ \frac{1}{L} \end{bmatrix}; C = [1 \ 0 \ 0]; D = [0] \quad (13)$$

Table 1: The parameters of the proposed MLS

Parameter	Value	Unit
m (mass)	0.0185	kg
g (gravitational acceleration)	9.8	m/s ²
R (internal resistance)	18.2	Ohm
L (inductance)	58.1m	H
c (magnetic force constant)	0.000058	-
y (ball position)	0.012	m
x ₀₂ (velocity of the ball)	0.0	m/s
(System is linear if this is equal to 0)		
i (current)	0.67	A

The physical parameters of the proposed magnetic MLS are presented in Table 1:

From the parameters acquired from the system, a state space model can be calculated based on Equation (13):

$$A = \begin{bmatrix} 0 & 1 & 0 \\ 816.67 & 0 & -29.21 \\ 0 & 0.111 & 313.25 \end{bmatrix}; B = \begin{bmatrix} 0 \\ 0 \\ 17.21 \end{bmatrix}; C = [1 \ 0 \ 0]; D = [0] \quad (14)$$

The transfer function obtained from the space state model is:

$$T(s) = \frac{-502.7}{s^3 + 313.2s^2 - 813.4s - 255800} \quad (15)$$

2.2 Model-Based Design in MATLAB/Simulink

A proportional-integral-derivative controller (PID controller) is also included in the block diagram to ensure the stability of a closed-loop control system. For this project, the PID controller is used to regulate the output voltage for the electromagnet to levitate the magnet positioned under the sensor and the electromagnet. A PID controller continuously calculates an error value $e(t)$ as the difference between a desired setpoint and a measured process variable and applies a correction based on proportional, integral and derivative terms (denoted K_p , K_i and K_d , respectively). The overall control function of the PID controller is expressed as:

$$u(t) = K_p e(t) + K_i \int_0^t e(t) d\tau + K_d \frac{d}{dt} e(t) \quad (16)$$

Based on the transfer function from Equation (15), a Simulink block diagram of the MLS has been created, as shown in Fig. 2:

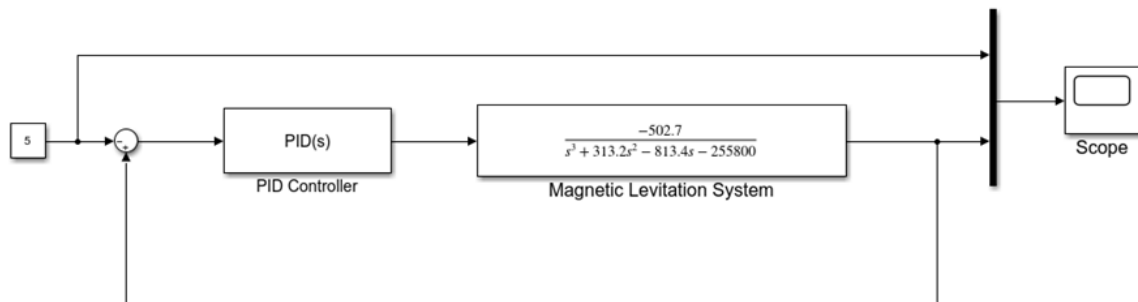


Fig. 2: Simulink block diagram of the MLS

2.3 Prototype Circuit Design

A 12V power supply is connected to the circuit to power up the magnetic levitation system. In contrast, the Arduino Mega can be powered up via the USB port while connected to a computer. The actuator consists of an electromagnet, a 1kΩ resistor, a diode and an NPN transistor. The transistor base is connected to the PWM digital pin, which acts as a switch to regulate and control the output current and voltage of the electromagnet. The Hall effect sensor is powered by a 5V pin and GND pin, while the OUT pin of the sensor is connected to an analogue pin of the Arduino Mega. The Arduino is programmed to increase the voltage when the neodymium magnet is far from the detection range, reduce the voltage when the magnet is too close, and levitate the magnet at a set point.

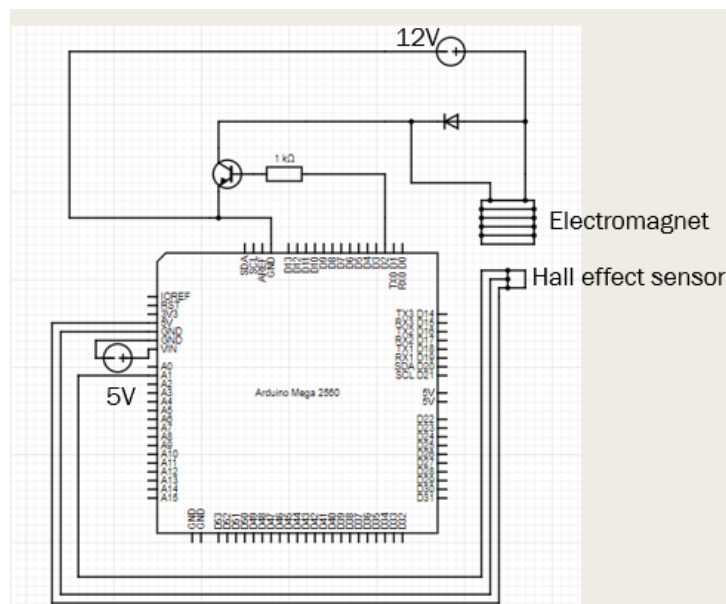


Fig. 3: Schematic diagram of the proposed circuit

3. RESULTS AND DISCUSSIONS

Fig. 4 shows the photograph of the experiment setup. The setup consists of a stand, which holds the electromagnet. A Hall effect sensor is attached about 5mm under the iron core of the electromagnet by placing a separator-like cardboard between the sensor and the electromagnet to reduce the influence of the magnetic field from the electromagnet. The electromagnet is connected to a breadboard, which houses the system circuitry. In contrast, the sensor is connected to Arduino Mega 2560, which returns magnetic field strength input to the Arduino. The circuit is connected to a 12V DC power supply. This magnetic levitation system prototype will be used in the experiment to test the PID gains acquired from the simulation in the Simulink block diagram.

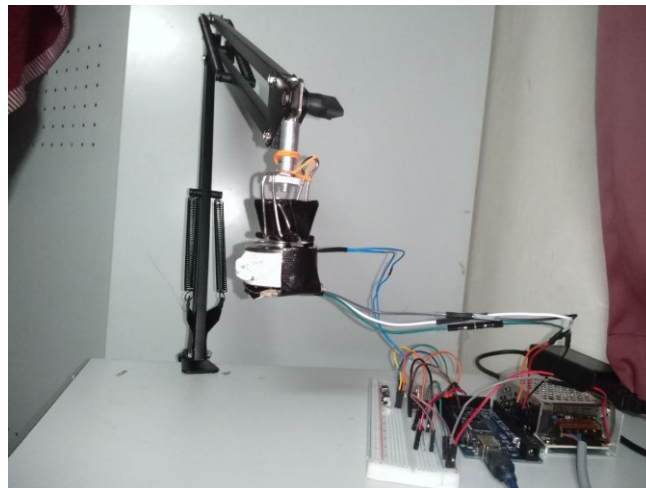


Fig. 4: Photograph of the experimental setup

3.1 Simulation Result

Firstly, the experiment starts with determining PID gains by simulating the block diagram from Fig. 2 in Simulink to generate a signal of the unit step response of the system. This was done using the PID Tuner App in Simulink to help the PID tuning process of a system much faster. The PID Tuner App automatically fills PID gains into the PID controller block parameter. The simulation is rerun to see the result:

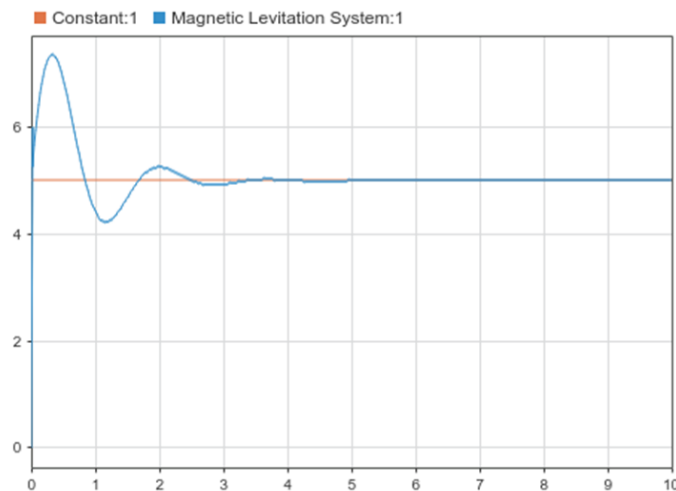


Fig. 5: Simulation result of the block diagram simulation

Based on the result above, when the values $P = 995.5$, $I = 2825.5$ and $D = 183.9$ are set into the PID controller, the system in the simulation becomes stable after passing its settling time at 2.5 seconds. To further test whether the PID gains generated by the Simulink software are entirely applicable to the real-life system, the PID gains are used in the source code for the Arduino Mega and uploaded into the controller with $K_p = 995.5$, $K_i = 2825.5$ and $K_d = 183.9$.

3.2 Arduino Serial Plotter Result

While testing the three values of PID gains into the Arduino Mega, the serial plotter from the Arduino IDE shows that the PID value increases way too much when the magnet is away from the sensor and decreases way too much when the magnet is close to the sensor, making it very hard for the system to stabilize. It shows that the PID gains are too high for the magnetic levitation system prototype. With high gains of PID, the increase and decrease of setpoints become harder to control, as shown in Fig. 6.

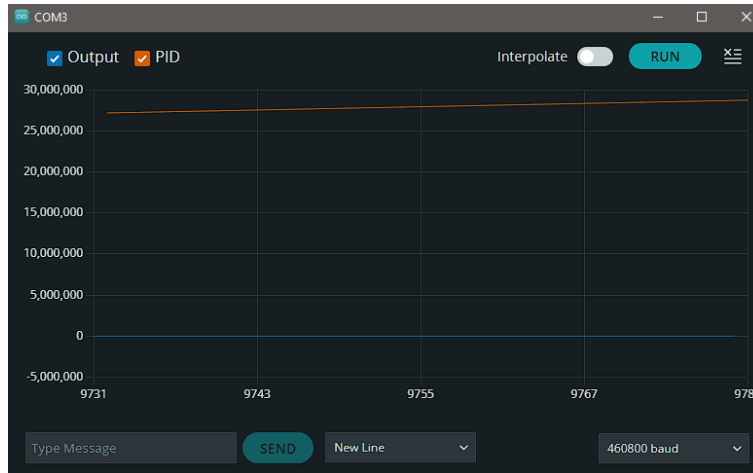


Fig. 6: Arduino serial plotter showing a very high gain in PID control function

To solve this issue, all the PID gains are reduced with a trial-and-error method to slow down its increase and decrease. The gains firstly are reduced by 10, followed by 100 and lastly 1000.

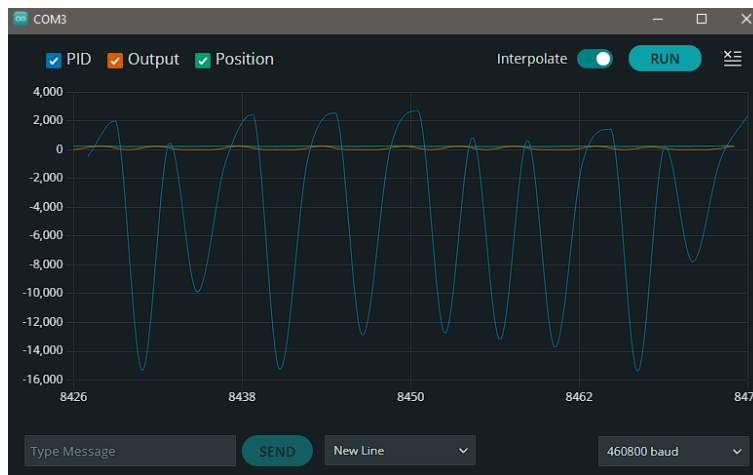


Fig. 7: PID control function after the PID gains are reduced by a factor of 10

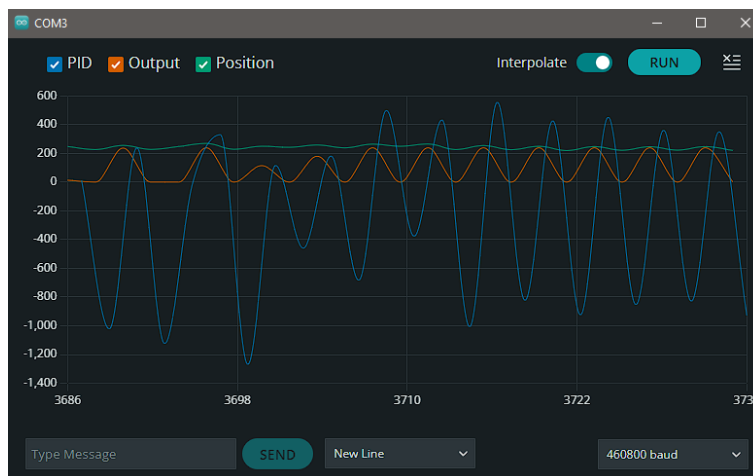


Fig. 8: PID control function after the PID gains are reduced by a factor of 100

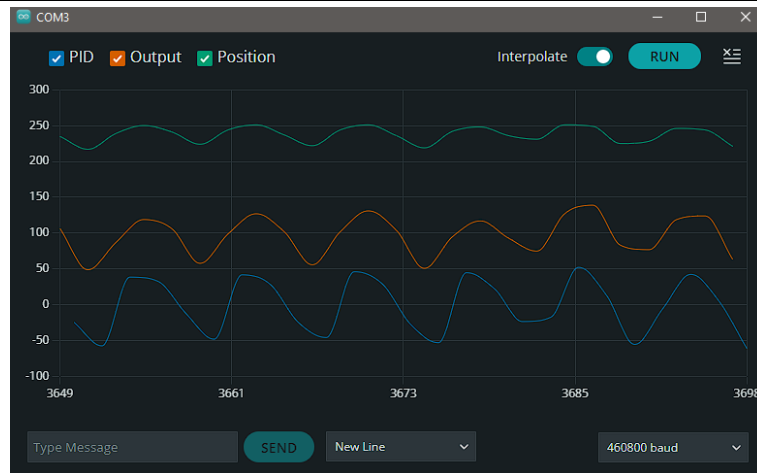


Fig. 9: PID control function after the PID gains are reduced by a factor of 1000

After the new PID gains, $K_p = 0.9955$, $K_i = 2.8255$ and $K_d = 0.1839$ are verified and uploaded into the Arduino, the Hall effect sensor measures an almost stable position of the permanent magnet.

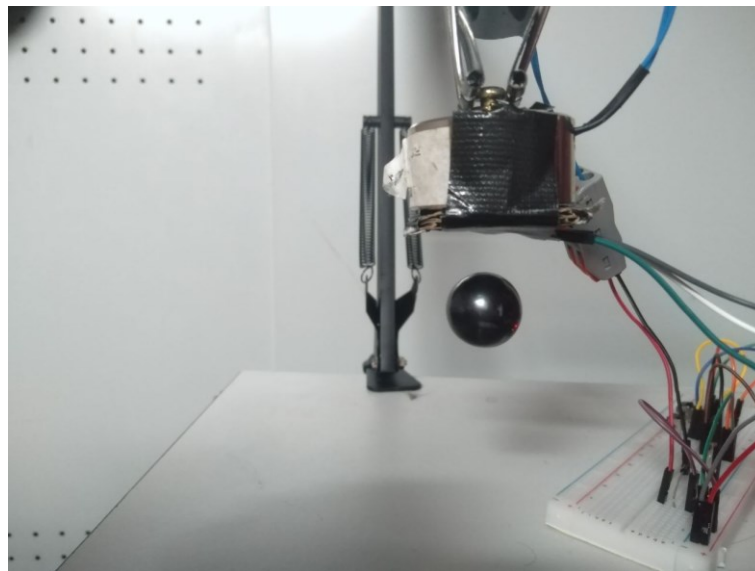


Fig. 10: MLS system with levitated ball magnet

4. CONCLUSION

This paper explores modelling a Magnetic Levitation System (MLS) through block diagram simulation in MATLAB/Simulink and controlling a real MLS using a digital PID controller implemented on an Arduino Mega. A simplified mathematical model was developed for the real system by measuring and identifying its components and hardware parameters. The project aimed to apply Proportional-Integral-Derivative (PID) control theory and program it into a functional, real-world prototype. After reducing the PID gains by 1000, the system achieved significant stabilization, resulting in the final gains of $K_p = 0.9955$, $K_i = 2.8255$, and $K_d = 0.1839$. However, minor oscillations were observed in the system due to external factors like the electromagnet overheating over time. Further finetuning of the PID gains may be necessary to minimize these oscillations.

REFERENCES

- [1] A. Abbas *et al.*, "Design and Control of Magnetic Levitation System," *1st Int. Conf. Electr. Commun. Comput. Eng. ICECCE 2019*, no. July, pp. 24–25, 2019.
- [2] S. M. R Rasid, M. B. Hossain, M. E. Hoque, M. A. A. Arif, and M. S. Ali Sarder, "Modeling and controlling a magnetic levitation system using an analogue controller," *Acta Electron. Malaysia*, vol. 3, no. 2, pp. 41–44, 2019.
- [3] P. Balko and D. Rosinova, "Modeling of magnetic levitation system," *Proc. 2017 21st Int. Conf. Process Control. PC 2017*, pp. 252–257, 2017.
- [4] J. de Jesús Rubio, L. Zhang, E. Lughofer, P. Cruz, A. Alsaedi, and T. Hayat, "Modeling and control with neural networks for a magnetic levitation system," *Neurocomputing*, vol. 227, pp. 113–121, 2017.
- [5] M. J. Khan, M. Junaid, S. Bilal, S. J. Siddiqi, and H. A. Khan, "Modelling, Simulation & Control of Non-Linear Magnetic Levitation System," 2018.
- [6] I. Ahmad, M. Shahzad, and P. Palensky, "Optimal PID control of Magnetic Levitation System using Genetic Algorithm," *Energycon 2014 - IEEE Int. Energy Conf.*, pp. 1429–1433, 2014.

Controlling the Variable Inertia of Flywheel: A Scientific Review

Muhammad Mahbubur Rashid* and Syed Munimus Salam

*Dept. Faculty of Mechatronics Engineering,
International Islamic University Malaysia, Kuala Lumpur, Malaysia.*

*Corresponding author: mahbub@iium.edu.my

(Received:28 February 2024; Accepted: 6 June 2024)

Abstract— Due to the variation of the moment of inertia, flywheels, a well-known mechanical system, can balance the energy output by preventing fluctuations in rotational speed. Examples of prevalent applications are the engine with internal combustion and industrial apparatus. A flywheel with a considerable moment of inertia is mandatory to accomplish reduced angular velocity variations. A flywheel with a variable moment of inertia can be recommended for specific applications to obtain sustainable energy savings. Variations in the masses' radii from the flywheel axis can yield the concept of true inertia. Still, the control techniques for the variable inertial flywheel (VIF) are relatively complex. This paper critically analyses the available literature on VIF control methods and focuses on their application.

Keywords: *VIF, MR Fluid, Flywheel, Smart Material.*

1. INTRODUCTION

Even though flywheels as mechanical devices have been used for many years to store brief energy spurts, it wasn't until the last century that they could store energy for relatively long durations. This device, which utilized the flywheel as its energy source, produced naval torpedoes with a high velocity and a long range. In addition, it was extremely precise due to the centrifugal stabilization, produced no disturbance, and did not modify trim [1]. The efficacy of flywheels has increased considerably over the past few decades, primarily due to the availability of anisotropic materials with improved strength-to-weight ratios. Since the energy-to-weight ratio of a flywheel is a direct consequence of the strength-to-weight ratio of the material used in its production [2], there has been a great deal of recent interest in the development of flywheel topologies that could best utilize the new family of anisotropic materials.

The energy-to-cost ratio of modern flywheels has also increased. Airspace organizations have completed a program that included flywheels made from unique, low-cost materials with a reasonable strength-to-weight ratio. Although in many low-cost flywheel applications, the weight or capacity of the flywheel has little impact on the system, the energy densities for the extremely low-cost flywheel program ranged from 22 to 44 Wh/kg [3]. Applying a large moment of inertia to a flywheel may cause difficulties during machine initiation. Any rotating machine with a large moment of inertia at start-up will have a high moment of inertia torque, which is inefficient. During high-speed, steady-state operation, this system's large moment of inertia conserves energy. Numerous published works propose a variable inertia flywheel to solve this issue.

The design of a flywheel with variable inertia must necessarily be more complex than that of a flywheel with constant inertia. The change of momentum of mass causes a change in inertia force that causes unwanted energy loss, resulting in a vibrating operation. Thus, as the reduction of stability, the unstable forces on the body cause undesirable vibration, which, depending on the machine configuration, can be torsional, linear, or bending. Vibration is a significant problem in any mechanical system that can impact the machine's service life, reduced quality, lack of safety, etc. [4]. Consequently, minimizing and controlling instability due to vibration is a crucial undertaking. The fundamental components of change in system stability are the spring components, used masses, and damping force of a damper. Important to the modelling of an effective vibration isolation system [5]-[6] includes the steps- the effective planning, system performance optimization, and accurate fabrication of these

three components.

Vibration is typically undesirable when it causes annoying commotion, results in peril, or dissipates energy. As a result, researchers have always been interested in vibration control. In the past few decades, vibration controlling, including passive systems and active or semi-active systems, were the primary focus of research. In these systems, system rigidity has a significant impact on the response of the system. The main consideration is to reduce the response time and to include a dynamic working range. The main benefit of a semi-active controlling system is the requirement for less external energy, which acts as the control energy and is sometimes considered an extra stability than that of active control. Therefore, semi-active control systems are fascinating and utilized in numerous engineering disciplines. For semi-active control, variables can be mass, rigidity, or damping [7]- [8].

A magnetic field may be used to regulate the viscosity of a family of intelligent materials known as magnetorheological (MR) materials [9]. These materials are made up of magnetically sensitive, non-colloidal particles, often iron or iron-carbide, suspended in a magnetically inert matrix material. A magnetic field causes the magnetic particles to form chain-like formations, raising the matrix's effective viscosity.

2. PAPER STRUCTURE

The variable inertia flywheel is a significant innovation that has revolutionised several industries because of the development of advanced technologies and cutting-edge methods. This paper aims to examine the variable inertia flywheel's structure, Control technique, application, simulation, challenges, and future potential.

The variable inertia flywheel is a mechanical device designed to store and discharge energy as efficiently as feasible. In contrast to conventional flywheels in a fixed moment of inertia, the variable inertia flywheel allows the user to alter the moment of inertia dynamically. Due to this characteristic, the device can adapt to different scenarios and optimize energy preservation and discharge based on specific applications' needs [10].

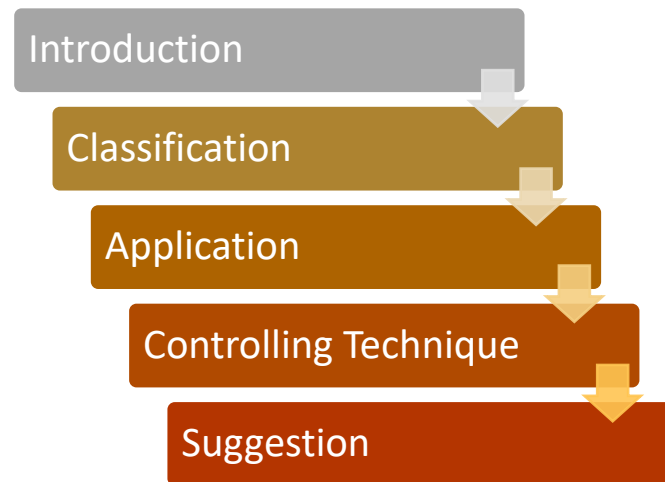


Fig. 1. Structure of the paper

Due to the coordination of its mechanical and control systems, the flywheel with varying degrees of inertia can execute its functions. A motor that can alter the location of the mass distribution is a component of a mechanical system that also consists of bearings and a rotating disc. The control system is accountable for moderating the motor's speed and position, as well as making any necessary adjustments to the flywheel's moment of inertia. This dynamic adjustment allows for exact control in the storage and discharge of energy.

3. CLASSIFICATION OF FLYWHEEL

A description of "VIF" and "FIF" are utilized to indicate two separate kinds of flywheels defined by the inertia characteristics they possess when discussing the classification of flywheels. Following is an explanation of the terms "Variable Inertia Flywheel" (VIF) and "Fixed Inertia Flywheel" (FIF). Flywheels with energy storage are sometimes incorporated into rotating apparatus to withstand sudden load changes.

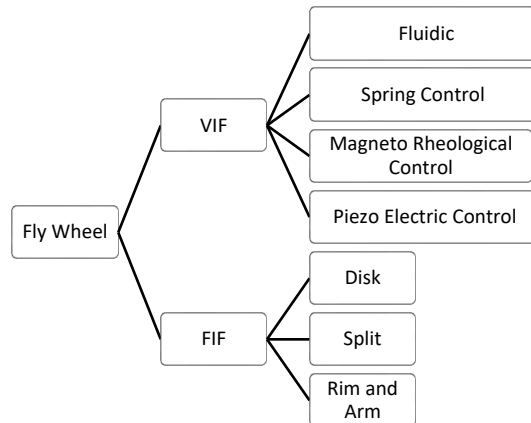


Fig. 2. Types of Flywheels according to inertia

Flywheels with fixed inertia (FIF) and flywheels with variable inertia (VIF) are the two primary varieties of flywheels used to store energy. Despite its widespread use due to its simplicity, FIF's high inertia causes machines to recover to their original speeds slowly. Researchers have debated and investigated the concept of VIF for many years. The control effects of VIF are substantially more potent and of much smaller magnitude than those of FIF. Its limited utility is due to its intricate construction and exacting maintenance. Reduced speed fluctuations in rotating apparatus are a relatively new research and application field [11]. Adaptive attitude control in spacecraft and the storage of electrical energy are two typical applications of VIF today.

3.1 Variable inertia flywheel (VIF)

The Inertia that varies in a Flywheel, as the name suggests, is a flywheel that allows for the dynamic adjustment of its moment of inertia. The resistance of a flywheel to a change in its spinning motion is its moment of inertia, which is determined by the distribution of the flywheel's mass. VIFs may have their moment of inertia modified to suit better their needs or the conditions in which they operate [12]. The flywheel's malleability in terms of its moment of inertia has several advantages. It allows for fine-grained management of energy storage and release, improving power transmission and the overall energy efficiency of a wide range of uses. VIFs may dynamically respond to changes in load or speed, enhancing the system's overall efficiency and responsiveness.

3.2 Fixed Inertia Flywheel (FIF)

In contrast to variable inertia flywheels, fixed inertia flywheels have an inertia moment that does not change while the flywheel operates. FIFs cannot dynamically adjust their inertia characteristics, and once their mass distribution is determined, it cannot be altered [13].

FIFs are often employed as a solution in applications that need a continuous and predictable spinning behavior. They provide dependable rotational energy storage and can serve as a kinetic energy reservoir, both supporting the effective operation of a range of systems. FIFs are often utilized when a fixed inertia is sufficient to meet the system's demands, such as internal combustion engines, industrial machinery, and power production [14].

4. VIF APPLICATION AND TECHNIQUE

In a flywheel with variable inertia, the slider's passage through the slot causes the flywheel's inertia to change. Fig. 3 depicts the conceptual design of the variable inertial flywheel. When the flywheel speed is zero, the springs are initially at their free length and contact the hub. Here, gravity's impact is disregarded. The springs can only be compressed; they cannot expand farther [15].

Elliott et al. presented a particular kind of VIF in which the mass block's displacement could be changed by the centrifugal force and its position could be fixed by the control system using primarily a hydraulic fluid along with

a control system including a valve [16]. Thus, a flywheel with variable inertia can increase the stability of equipment at high speeds by starting with a little inertia; on the other hand, a high-speed rotation with a large inertia but requires a suitable controlling system, where the moment of inertia is protected by the inserted hydraulic fluid. Another VIF introduced, which gain the variation of inertia by controlling the valve of fluid flow, was suggested by Dugas [17]. By filling and emptying, Jayakar et al. [18] found that the VIF's inertia could be altered by utilizing any viscous fluid characteristics.

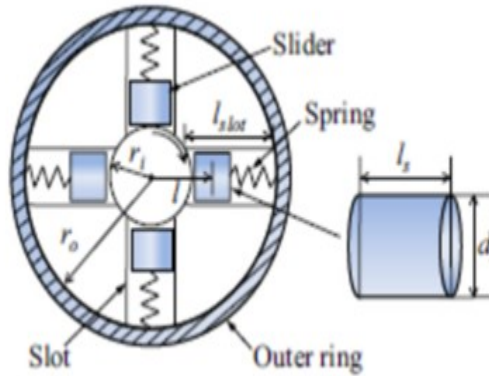


Fig. 3. Schematic presentation of VIF[15]

The VIF can reduce fluctuations in the speed of the engine brought on by the power demand change by managing the fluid in the chamber, but this is challenging since fluid must be filled and managed. The idea of a flywheel with a variable moment of inertia has been demonstrated using a container with an engineered shape; as the liquid inside disperses at increasing speeds, the moment of inertia changes from that of a disk-type flywheel to a hoop-type flywheel, all three of which are constrained to the same mass and outer radius. The percentage of extractability improves by more than 10%, even if the amount of energy that can be extracted within the specified speed range is equivalent to that of a flywheel with a hoop-like design.

Additionally, the amount of wasted energy that remains below the lower speed restriction is cut in half. Despite the demonstration flywheel's limitations in terms of practicality, J. Barid et al.'s Design of a Liquid-Based Variable Inertia Flywheel provides a design technique and numerous future factors. [19]. The moment of inertia of the slider about its own mass center and that of the fixed structural part about the shaft center, respectively, are expressed as

$$J_s = \frac{1}{4} M_s \left(\frac{d_s^2}{4} + \frac{l_s^2}{3} \right) \dots \dots \dots (1)$$

$$J_F = J_{shaft} + J_{scd} - N J_{slot} \dots \dots \dots (2)$$

where,

$J_{scd} = \frac{1}{4} M_{scd} (r_s^2 + r_o^2)$ is the polar moment of inertia of a solid flywheel of uniform thickness

J_{shaft} is the polar moment of inertia of the shaft

$$J_{slot} = m_{slot} \left\{ \frac{1}{12} (d_s^2 + l_{slot}^2) + (r_o + .5 l_{slot})^2 \right\} \dots \dots \dots (3) [15]$$

A pre-compressed spring is set between the piston and the frame. The coil is entangled in the double ring groove of the piston. If we consider friction force F_f , the spring force F_0 , MR damping force F_{mrf} , $\sin w$ is a sign function related to the radial slip velocity of piston and k is the spring constant

$$J_{slot} = m_{slot} \left\{ F_0 + (F_{mrf} + F_f) \sin w + k \frac{r_i}{m_{slot} \omega^2 - k} \right\} \dots \dots \dots (4) [20]$$

A fluid was used to operate as a succession of inertia masses in L. Islam's proposal for a novel vibration suppression system that uses changeable inertia mass [21]. S M Salam focuses the VIF utilization in rotating

machine to reduce energy consumption by simulation [22]. The addition of MR fluid can improve the research as well. However, there hasn't been much practice using magnetorheological fluid to create changing inertia in a flywheel. Variable inertia magnetorheological flywheels (VIMRF) have yet to be fully investigated regarding their potential for energy savings.

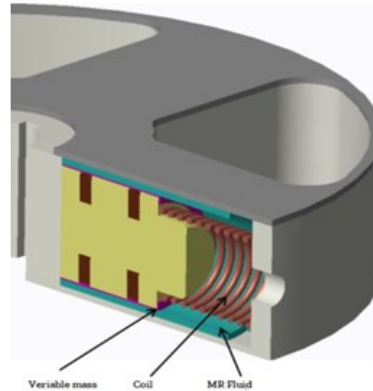


Fig. 4. VIF with MR Fluid[20]

The VIF prototype is shown in Fig. 5. There are sixteen sliding rods inserted around the flywheel's center, with a mass block and a spring on each sliding rod, spaced every two rods. The mass block is connected to the flywheel center via the spring. When the sliding rod is placed into the mass block's holes, the mass block may move easily. The viscous damper of the mass block is formed by the airtight plate, and the viscous coefficient of the mass block is adjusted using the air holes on the side cover [23].

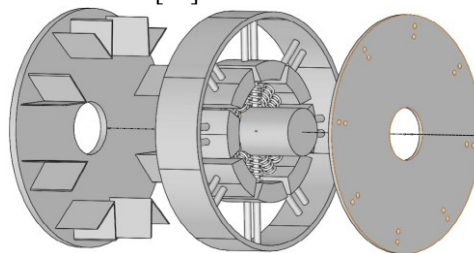


Fig. 5. VIF used for DG [23]

WEH consists mostly of the transmission system, mechanical motion rectifier, generator connected with VIF, circuitry, and ancillary components in Fig. 16. While operating in the ocean, the buoy's up-and-down motion in response to wave excitation is considered the transmission module's vibration input. The ball screw transmission module transforms recompensing vertical motion to recompensing rotation. During transmission, the mechanical motion rectifier turns the reciprocating rotation to a one-direction rotation via clutches and boosts the angular velocity. The VIF can store or release energy to stabilize the generator's speed and enhance its effectiveness. Lastly, the AC generator produces electricity, which either powers the load or is stored in a capacitor.

4.1 VIF In Wave Energy Converter

The VIF's inertia is the wheel's constant and the mass blocks' variable. Spring-pushed mass blocks and four cantilever sliders lessen initial torque. The mass blocks' rotation radius r rises when accelerating due to centripetal force and decreases when decelerating due to spring force, resulting in a smoother velocity shift and longer overrunning phase. When modelling the increased output voltage of the WEH after including the VIF, it is important to account for the overrunning period of the mechanical motion rectifier. The rotational speed, m , of the generator at a single instant, T , is modelled. (Fig. 6). The WEH overrunning phase without VIF varies between 0.11 T and 0.32 T for 0.50 Hz and 25 mm amplitude and between 0.03 T and 0.40 T with VIF. The duration is lengthened, and its velocity diminishes gradually. Due to overrunning, it is estimated that the mechanical motion rectifier contributes 16% to the rise in output voltage, while the VIF puts up an added 25%. So, the output benefits from the VIF's ability to cut down on velocity attenuation in a streamlined fashion.

The WEH has been tested both with and without VIF setup to determine its effectiveness. The input force is measured with and without VIF during the meshing phase. However, during the overrunning period, the rise in input force with VIF is slowed (Fig. 6a) because the overrunning period with VIF is longer than without VIF.

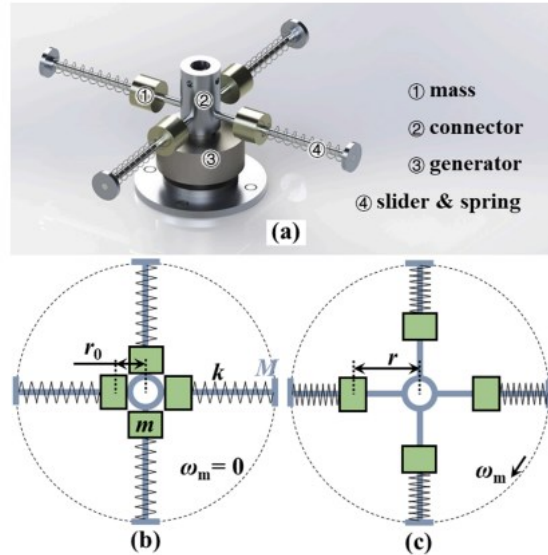


Fig. 6. Design of the VIF. (a) The structure of the VIF. (b) Normal state (c) Operating state [24]

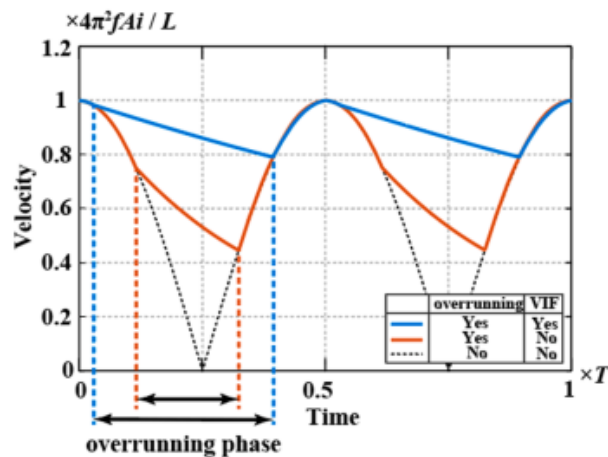


Fig. 7. Simulated angle of rotation of the generator [24]

In addition, the output voltage with VIF is greater than in the absence of VIF during the overrunning period (Fig. 6 b). After integrating the voltage curve (Figure 6b), the expansion of the overrunning period raises the output voltage by 8.2%, while with VIF, it increases by 13.5% in output power and 25.5% in efficiency. The highest output power is 2.15 W, the average output power is 1.17 W, and the efficiency is 51.54%.

4.2 VIF in Power Utility

A flywheel with balanced positioned dampers was utilized in a ball screw-type power takeoff system. Due to their ability to change inertia, small mass spring dampers can be cost-effectively adapted to the system's conditions. In addition to the passive configuration, partially active and active configurations are proposed to improve the system's efficiency and expand its functional extent [25].

4.3 VIF In Spacecraft System

In the design of a diesel-producing unit that experiences pulsed load, the traditional fixed inertia flywheel (FIF) is replaced by a variable inertia flywheel (VIF). FIF is commonly utilized due to its easy-to-build design, however, its high inertia causes the speed to restore steadily to its original value. VIF's size is significantly reduced but its control effects are much increased in comparison to FIF. However, its complicated design and laborious routine maintenance prevent it from seeing widespread use. Presently, VIF is mostly applied to the adaptive attitude control of spacecraft and the storage of electric energy; it is rarely employed to reduce the speed fluctuations of spinning gear [26].

4.4 VIF In Wind Energy Converter

A wind turbine's rotor blades are loaded with mass that increases the rotor's moment of inertia. This flywheel's inertia can be adjusted by repositioning the weights near to the center of the flywheel. It has a traditional drivetrain with a transmission and a rapidly spinning generator. In the literature, different designs of these wind power generators are explained in considerable attribute. Simulating the beginning part-load operation with constant wind speed shows the flywheel system's behavior. In the second situation, the turbine operates at partial load when wind speed temporarily meets its rated value. Comparisons are made with and without the flywheel. In the third instance, the same approach is followed when the turbine is operating at full load, and a temporary fall in wind speed causes the wind turbine's output to diminish. The wind power generator operates at a partial load while the speed of the wind remains constant. For the flywheel to turn, its mass must be transferred from the smallest to the biggest radius and then back to the smallest [27][28].

4.5 VIF In Breaking System

Figliotti and Gomes proposed a VIF mechanism for bicycle restorative braking systems. Most transportation energy storage methods are either chemical or electrical in nature. Most purely mechanical energy conservation systems are capable of absorbing and releasing small amounts of energy over extremely brief timeframes. These systems are ideally suited for use as restorative decelerating systems for vehicles for high-rate energy transfer. Bicycles with regenerative braking systems were created using springs. However, flywheels are more desirable than mechanical springs because they may be configured to have larger power densities [29].

4.6 VIF In Vibration Reducer

In order to improve the effectiveness of passive vehicle suspension, it is proposed to employ a vibration absorber based on a two-terminal mass (TTM) with a variable moment of inertia (VMI). Sliders in a hydraulically powered flywheel do the VMI for the system. In reaction to strong vertical oscillations, the vehicle's moment of inertia grows, while weak vertical oscillations cause the moment of inertia to shrink. By means of a hydraulic mechanism, the system transforms the linear motion between the two suspension terminals into a rotational motion of the flywheel. Due to centrifugal force, the sliders inside the flywheel travel away from the flywheel's Centre when the vertical oscillation of the vehicle is greater, increasing the moment of inertia. When a car's oscillation is weaker, the opposite is true. Therefore, the moment of inertia can be adjusted to suit the conditions of the road. Dynamic modelling, simulation, and experimental investigation have been used to study the performance of the proposed TTM-VMI absorber. Besides sinusoidal excitations, the proposed VMI system exceeds its constant moment of inertia equivalent regarding response time, road handling and safety, ride comfort, and suspension bend [30].

4.7 VIF in Engine Performance Enhancement

Electrical landing gear of aerospace system drives, outfitted via traction motors, enable the tires of single-aisle passenger aircraft to be powered, allowing them to travel on the runway. The implementation of powered wheels addresses the issues of low engine efficiency, excessive fuel consumption, and elevated pollutant levels in the aircraft during the taxiing operation. The powered wheel electric drive system comprises an electric traction motor, a set of planetary gear assemblies, and a wheel. This research aims to enhance the torque output of the powered wheel by optimizing the characteristics of the planetary gear assembly in the electric drive system. Subsequently, two testing protocols are devised to quantify the torque of the powered wheel electric drive system.

These two test schemes utilize moments of inertia and resistance loading to simulate the real vertical load of the aircraft on the powered wheel during the taxiing procedure. The initial plan uses a mass block to replicate the mass of the typical aircraft. In contrast, the second scheme utilizes a flywheel with an adjustable moment of inertia to approximate the bulk of sizable commercial aircraft. [32].

Table 2. Variable Inertia Flywheels and their applications

VIF Components	Applications	Enhancement
Mass spring damper based VIF	Power hydraulic motor system	Motor efficiency increment
4 Slider based VIF	Diesel Generator Unit under Pulsed Load	Diesel Generator output power quality and efficiency improvement
Actively controlled VIF	Wave energy converter	Energy harvesting and performance acceleration
Band VIF	Urban transit bus	Efficiency increment
Four cantilever sliders base VIF	Wave energy harvester	Energy harvesting and performance acceleration
Mass spring damper based VIF	Regenerative Braking on A Bicycle	Breaking system performance enhancement
4 Slider based VIF	Hybrid Power Systems	Power quality and efficiency improvement
Mass spring damper based VIF	Hydraulic drive	Motor efficiency increment
4 Slider based VIF	Passive Vehicle Suspensions	Improvement of suspension system

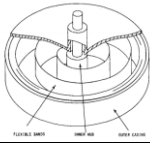
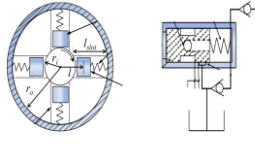
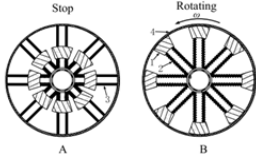
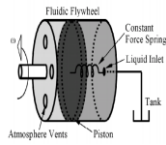
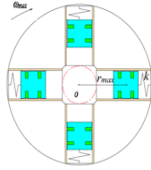
5. CONTROL STRATEGIES FOR VARIABLE INERTIA

Small mass spring dampers may be used to change the equivalent mass and associated parameters of economically and dynamically adaptable systems with variable inertia and mass amplification effects. In addition to the passive configuration, semi-active and active configurations are also provided to improve performance and widen the proposed VIF system's functional range. The dynamics of a flywheel with variable inertia have been revealed by numerical simulations, which have also shown its potential and confirmed its ability to adapt to different wave conditions.

In a passive design, mass-spring-dampers are evenly distributed throughout the flywheel plate; in a semi-active configuration, the mass may be temporarily locked at its origin; in an active configuration, the spring stiffness can be adjusted. Refer to Figure 6; the setups of VIF are described with different conditions especially passive, active, and semi-active state. Additional switches are introduced for the mass-spring dampers for the semi-active VIF. Semi-active VIF is like passive VIF while the switches are off; when the switches are activated, the mass will

remain locked at its origin. The mass-spring dampers in symmetric places will be simultaneously locked to maintain the VIF's balance [33]. The Semi-active devices cannot directly input energy into the system they control. This crucial requirement ensures that system parameter changes do not result in parametric excitation [34]. When employing the word "semi-active" in literature, this is often not taken into appropriate consideration. It has been shown to function better than a passive control system and is utilized as one effective method to reduce unwelcome vibrations in many applications.

TABLE I: MAJOR VIF CONTROL TECHNOLOGIES.

Technology	Schematic Figure	Findings
Band-type variable inertia flywheel		BVIF-integrated systems save 30% on fuel. Regenerative braking reduces brake wear by five times.
Hydraulic flywheel system with two terminals for variable moment of inertia		The variable inertia flywheel was analyzed using a two-terminal hydraulic system. Experimentally determined hydraulic device and variable inertia flywheel parameters.
Spring		The variable moment of inertia flywheel stabilizes diesel generator speed under loads. SIMULINK simulations show that the variable inertia flywheel reduces diesel generator loading impact.
Fluidic Variable Inertia Flywheel		Experimental evidence suggests that the fluidic flywheel can keep its angular velocity constant despite having a mass moment of inertia that is one order of magnitude smaller than that of a traditional flywheel.
Magneto-rheological fluid based variable inertia flywheel		MRVIF is created and tested for semi-active adjustment. The maximum allowable range for adjusting inertia is 27.2%.

Active vibration control is, however, overshadowed by the system's relative expense, complexity, and instability [35]. Semi-active dampers are hydro-mechanical control mechanisms that can change how much energy they release while drawing just a small amount of electricity. Magneto-rheological fluid (MRF) is the term used to describe the resulting combination, which is most often [36] a fluid. Elastomers may also be employed as matrix material because of their increased viscosity when no magnetic field exists [37]. There are also magnetorheological foams, in which a spongy substance, such as a metal foam, is soaked in an MRF or MR elastomer [38]. Magnetic particles, base fluids, and additives are the three primary elements of MRF [39]. The magnetically active component is made up of magnetic particles, which produce patterns resembling chains when exposed to a magnetic field. In addition to serving as a carrier and lubricant, the base fluid also offers traditional damping. The use of additives improves numerous qualities, including friction, corrosion, sedimentation, and viscosity. The behavior of the fluid during active, semi-active or passive state has an impact on the improvement of these qualities [40][41].

VIF is one of the common concepts that utilized the effect of moment of inertia in a flywheel system. It is difficult to control the mass in the VIF as there is a change in momentum of the mass. Previously different fluidic VIFs is used for improvement in design of a VIF [16] [17] [18][42][45]. The main objective of these design variations is to save energy requirements. Some VIF concepts are also utilized to harvest energy [24], where the spring and semi-active fluid is used to get optimum output. Many literatures focus their research on reducing the unwanted vibration using VIF in diesel generation power production. Most of the systems used for VIF mass controlling are passive type and some are semi active. Only a few used with active control but little cost benefit achieved [43][44].

6. CONCLUSION

Though there are semi-active fluids like MR fluid that can be used to improve control, most of them used for energy harvesting and vibration control in power production. There is a new concept developed by Yang et al to use MR fluid for controlling the power consumption of rotating electrical machines but only theoretically proved. The application of electrical rotating machine power consumption optimisation can be another interesting topic for VIF application. Also, the utilisation of different smart material in MRF and ERF also explores a new horizon in the applied side. According to inertia control science, the semi-active Controller has potential applications that other vibration control does not. The most apparent are the civil construction and automobile industries, which currently employ controllers. There may be more that haven't been considered, however. Considering the prospect of utilising semi-active controllers as vibration absorbers for constructions whose inherent frequency varies over time is exciting. One example is vibration absorbers for VIF that adjust to the increasing mass when loaded. Finally, it seems that this is a promising field for the design of governing mechanisms in general and that it will help us better understand their limits.

REFERENCES

- [1] J. A. Kirk, "Flywheel energy storage—I," *Int J Mech Sci*, vol. 19, no. 4, pp. 223–231, Jan. 1977, doi: 10.1016/0020-7403(77)90064-9.
- [2] D. Ullman and H. Velkoff, "An introduction to the variable inertia flywheel (VIF)," *Journal of Applied Mechanics, Transactions ASME*, vol. 46, no. 1, pp. 186–190, 1979, doi: 10.1115/1.3424494.
- [3] X. Li and A. Palazzolo, "A review of flywheel energy storage systems: state of the art and opportunities," *J Energy Storage*, vol. 46, p. 103576, Feb. 2022, doi: 10.1016/j.est.2021.103576.
- [4] C. Li, M. Liang, and T. Wang, "Criterion fusion for spectral segmentation and its application to optimal demodulation of bearing vibration signals," *Mech Syst Signal Process*, vol. 64–65, pp. 132–148, Dec. 2015, doi: 10.1016/j.ymsp.2015.04.004.
- [5] D. Richiedei, A. Trevisani, and G. Zanardo, "A Constrained Convex Approach to Modal Design Optimization of Vibrating Systems," *Journal of Mechanical Design*, vol. 133, no. 6, Jun. 2011, doi: 10.1115/1.4004221.
- [6] C. E. Spiekermann, C. J. Radcliffe, and E. D. Goodman, "Optimal Design and Simulation of Vibrational Isolation Systems," *American Society of Mechanical Engineers (Paper)*, 1984.
- [7] Y. Liu, "Semi-active damping control for vibration isolation of base disturbances," *Diss. University of Southampton*, 2004.
- [8] M. Trikande, N. Karve, R. Anand Raj, V. Jagirdar, and R. Vasudevan, "Semi-active vibration control of an 8x8 armored wheeled platform," *Journal of Vibration and Control*, vol. 24, no. 2, pp. 283–302, Jan. 2018, doi: 10.1177/1077546316638199.
- [9] J. D. Carlson and M. R. Jolly, "MR fluid, foam and elastomer devices," *Mechatronics*, vol. 10, no. 4, pp. 555–569, 2000, doi: 10.1016/S0957-4158(99)00064-1.
- [10] P. M. V. Kartašovas, V. Barzdaitis, "Modeling and simulation of variable inertia rotor," *J. Vibroengineering*, vol. 4, pp. 1745–1750, 2012.
- [11] Masahiro Yamazaki, "Variable Mass Flywheel Mechanism: USA," *US 6915720 B2*, 2005.
- [12] K. D. Prabhakar Kushwaha, Sanjoy K Ghoshal, "Dynamic analysis of a hydraulic motor drive with variable inertia flywheel," *J Systems and Control Engineering*, vol. 234(6), pp. 734–747, 2020.
- [13] M. I. Daoud, A. S. Abdel-Khalik, A. Massoud, S. Ahmed, and N. H. Abbasy, "On the development of flywheel storage systems for power system applications: A survey," in *Proceedings of the 2012 XXth International Conference on Electrical Machines, France*, pp. 2119–2125: Marseille, Sep. 2012, pp. 2–5.

-
- [14] L. Barelli et al., "Flywheel hybridization to improve battery life in energy storage systems coupled to RES plants," *Energy*, vol. 173, pp. 937–950, 2019.
- [15] A. C. Mahato, S. K. Ghoshal, and A. K. Samantaray, "Influence of variable inertia flywheel and soft switching on a power hydraulic system," *SN Appl Sci*, vol. 1, no. 6, p. 605, Jun. 2019, doi: 10.1007/s42452-019-0623-0.
- [16] Uddin, M. N., M. M. Rashid, M. G. Mostafa, H. Belayet, S. M. Salam, and N. A. Nithe. "Global energy: need, present status, future trend and key issues." *Global Journal of Research In Engineering* 16, no. 1 (2016).
- [17] M. N. Uddin, M. M. Rashid, M. T. Rahman, B. Hossain, S. M. Salam and N. A. Nithe, "Custom MPPT design of solar power switching network for racing car," 2015 18th International Conference on Computer and Information Technology (ICCIT), Dhaka, Bangladesh, 2015, pp. 11-16, doi: 10.1109/ICCITech.2015.7488034.
- [18] S. K. Jayakar, Vijayaselvan, Das, "Variable Inertia Flywheel," 2012
- [19] J. Braid, "Conceptual design of a liquid-based variable inertia flywheel for microgrid applications," *ENERGYCON 2014 - IEEE International Energy Conference*, no. 2, pp. 1291–1296, 2014, doi: 10.1109/ENERGYCON.2014.6850589.
- [20] X. Dong, J. Xi, P. Chen, and W. Li, "Magneto-rheological variable inertia flywheel," *Smart Mater Struct*, vol. 27, no. 11, p. 115015, Nov. 2018, doi: 10.1088/1361-665X/aad42b.
- [21] L. Islam, M. M. Rashid, and M. A. Faysal, "Investigation of the Energy Saving Capability of a Variable Inertia Magneto-Rheological (MR) Flywheel," vol. 2, no. 1, pp. 25–31, 2022.
- [22] S. M. Salam and M. M. Rashid, "A new approach to analysis and simulation of flywheel energy storage system," in *8th International Conference on Mechatronics Engineering (ICOM 2022)*, Institution of Engineering and Technology, 2022, pp. 90–94. doi: 10.1049/icp.2022.2271.
- [23] Y. Zhang, X. Zhang, T. Qian, and R. Hu, "Modeling and simulation of a passive variable inertia flywheel for diesel generator," *Energy Reports*, vol. 6, pp. 58–68, 2020, doi: 10.1016/j.egy.2020.01.001.
- [24] Q. L. Yiqing Yang *, Peihao Chen, "A wave energy harvester based on coaxial mechanical motion rectifier and variable inertia flywheel," *Appl Energy*, vol. 302, 2021.
- [25] Q. Li, X. Li, J. Mi, B. Jiang, S. Chen, and L. Zuo, "Tunable Wave Energy Converter Using Variable Inertia Flywheel," *IEEE Transactions on Sustainable Energy*, vol. 12, no. 2, pp. 1265–1274, Apr. 2021, doi: 10.1109/TSTE.2020.3041664.
- [26] S. M. Salam, M. I. Uddin and M. R. Bin Moinuddin, "Impact Analysis of Large Number of Non-Linear Lighting Loads on Power Quality in Distribution Network," 2019 4th International Conference on Electrical Information and Communication Technology (EICT), Khulna, Bangladesh, 2019, pp. 1-5, doi: 10.1109/EICT48899.2019.9068811.
- [27] L. G. Yuan, F. M. Zeng, and G. X. Xing, "Research on the design and control strategy of variable inertia flywheel in diesel generator unit under pulsed load," in *2010 International Conference on Computing, Control and Industrial Engineering, CCIE 2010, Control and Industrial Engineering, 2010*, pp. 187–189. doi: 10.1109/CCIE.2010.55.
- [28] C. Jauch, "Controls of a Flywheel in a Wind Turbine Rotor," *Wind Eng.* 2016, vol. 40, pp. 173–185.
- [29] Figliotti MP and Gomes MW, "A variable-inertia flywheel model for regenerative braking on a bicycle," *ASME 2014 dynamic systems and control conference*, San Antonio, New York: American Society of Mechanical Engineers.
- [30] T. Xu, M. Liang, C. Li, and S. Yang, "Design and analysis of a shock absorber with variable moment of inertia for passive vehicle suspensions," *J Sound Vib*, vol. 355, pp. 66–85, 2015, doi: 10.1016/j.jsv.2015.05.035.
-

-
- [31] A. C. Mahato, S. K. Ghoshal, and A. K. Samantaray, Influence of variable inertia flywheel and soft switching on a power hydraulic system, vol. 1, no. 6. Nat. Appl. Sci 1: Springer, 2019. doi: 10.1007/s42452-019-0623-0.
- [32] M. Huang, "Optimization of powered wheels for commercial aircraft and design of test scheme," Proceedings of the Institution of Mechanical Engineers, Part D: Journal of Automobile Engineering, vol. 237, no. 7, pp. 1751–1764, Jun. 2023, doi: 10.1177/09544070221093182.
- [33] Q. Li, X. Li, J. Mi, B. Jiang, S. Chen, and L. Zuo, "Tunable Wave Energy Converter Using Variable Inertia Flywheel," IEEE Transactions on Sustainable Energy, vol. 12, no. 2, pp. 1265–1274, 2021, doi: 10.1109/TSTE.2020.3041664.
- [34] A. Preumont, "Vibration Control of Active Structures," Springer, 3rd edition, 2011, doi: 10.1007/0-306-48422-6.
- [35] S.-G. Luca, F. Chira, and V.-O. Rosca, "Passive Active and Semi-Active Control Systems in Civil Engineering," Constructil Arhitectura, vol. 3, p. 4, 2005.
- [36] M. J. Wilson, A. Fuchs, and F. Gordaninejad, "Development and characterization of magnetorheological polymer gels," J Appl Polym Sci, vol. 84, no. 14, pp. 2733–2742, 2002, doi: 10.1002/app.10525.
- [37] X. H. Liu, P. L. Wong, W. Wang, and W. A. Bullough, "Feasibility study on the storage of magnetorheological fluid using metal foams," J Intell Mater Syst Struct, vol. 21, no. 12, pp. 1193–1200, 2010, doi: 10.1177/1045389X10382585.
- [38] E. J. R. Hardy, "The magnetic fluid clutch," Students Quarterly Journal, vol. 22, no. 86, p. 51, 1951, doi: 10.1049/sqj.1951.0064.
- [39] W. Lu, Y. Luo, L. L. Kang, and D. Wei, "Characteristics of magnetorheological fluids under new formulation," J Test Eval, vol. 47, no. 4, 2019, doi: 10.1520/JTE20170477.
- [40] A. G. Olabi and A. Grunwald, "Design and application of magneto-rheological fluid," Mater Des, vol. 28, no. 10, pp. 2658–2664, 2007, doi: 10.1016/j.matdes.2006.10.009.
- [41] Z. Xia, X. Wu, G. Peng, L. Wang, W. Li, and W. Wen, "A novel nickel nanowire based magnetorheological material," Smart Mater Struct, vol. 26, no. 5, 2017, doi: 10.1088/1361-665X/aa5bd0.
- [42] James. Van de Ven, "Fluidic Variable Inertia Flywheel," 7th international energy conversion engineering conference, 2009.
- [43] M. H. Yousefi-Koma, Aghil, "Active Vibration Control of Flywheel Bearing Using Piezo Sensor-Actuator".
- [44] Uddin, Md Nasir, M. M. Rashid, M. G. Mostafa, H. Belayet, S. M. Salam, and N. A. Nithe. "New Energy Sources: Technological Status and Economic Potentialities." Global Journal of Science Frontier Research 16, no. 1 (2016): 24-37.
- [45] S. M. Salam, N. Mohammad and F. Hossain, "A new approach to Analysis the Impact of Demand Side Management for Temperature Control Load Consideration in a Test Bus System," 2021 5th International Conference on Electrical Information and Communication Technology (EICT), Khulna, Bangladesh, 2021, pp. 1-6, doi: 10.1109/EICT54103.2021.9733717.
-

Design of a Wilkinson Power Divider with Harmonic Suppression for Mobile Application

Hanis Humaira Iskandar Tuah* and AHM Zahirul Alam

*Department of Electrical and Computer Engineering,
International Islamic University of Malaysia,
Kuala Lumpur, Malaysia*

*Corresponding author: hanishumaira09@gmail.com

(Received: 28 February 2024; Accepted: 6 June 2024)

Abstract—This paper presents a Wilkinson Power Divider (WPD) operating at 6 GHz capable of suppressing unwanted harmonics up to the 3rd harmonic. The design formulas are analysed and presented in detail. Power dividers are widely used in microwave circuit structures. Indeed, this paper outlines the design and simulation of a 1:1 power divider for mobile applications using CST Studio Suite.

Keywords: *Wilkinson power divider, microwave, equal power division, and harmonic suppression.*

1. INTRODUCTION

The Wilkinson Power Divider, designed primarily for mobile applications, is a critical component in radio frequency (RF) systems, distributing RF power to various output ports with equal amplitude. In the world of mobile applications, the design of a Wilkinson Power Divider requires advanced considerations, balancing power division accuracy, bandwidth needs, and, most importantly, harmonic suppression. The Wilkinson Power Divider for mobile applications is designed not only to efficiently split the incoming RF signal but also to minimise harmonic production, which can affect signal quality and regulatory compliance. Harmonic suppression in the Wilkinson Power Divider requires optimising important parameters, such as resistor values and transmission line lengths, frequently using simulation tools like CST Studio Suite to eliminate undesirable harmonics.

They are commonly used as essential components in various microwave applications for power distribution and synthesis. The Wilkinson Power Divider is particularly favoured for its high return loss, excellent isolation, and low insertion loss, all achieved through a simple design. In the following sections, we will examine the design process of the proposed equal Wilkinson Power Divider in detail.

2. DESIGN OF WILKINSON POWER DIVIDER AND ITS PARAMETERS

This paper proposes designing a 1:1 Power Divider using CST Studio Suite software. Thus, a conception of a Wilkinson Power Divider with a ratio of 1:1 is presented at a central frequency of about $f_0 = 6$ GHz.

2.1 Design of a Wilkinson Power Divider

In this section, Figure 1 shows the proposed design of the Wilkinson Power Divider after it has been optimised by simulating CST Studio Suite software.

From this figure, the WPD is designed based on this dimension at a length of 40 mm and width of 50 mm. The substrate material used is Rogers RO4350B with a dielectric constant of 3.66. The thickness of the substrate is set to be 1.524 mm with a loss tangent of 0.0037. The lower the loss tangent, the better the performance of the Wilkinson Power Divider.

2.2 Design of Wilkinson Power Divider with Harmonic Suppression

Fig. 2 shows the method of suppressing the harmonics by cutting some of the copper parts to the ground. It also illustrates the dimensions of the cutting slot at the centre of the ground copper plate, with 8mm X 40mm representing length and width, respectively.

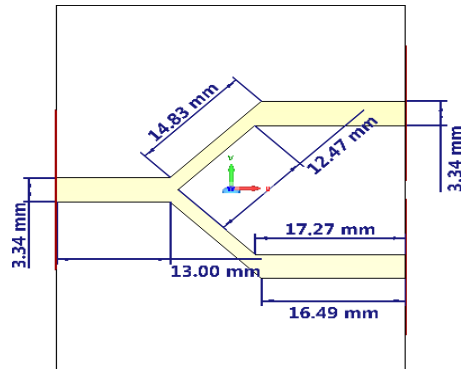


Fig. 1. Design of Wilkinson Power divider

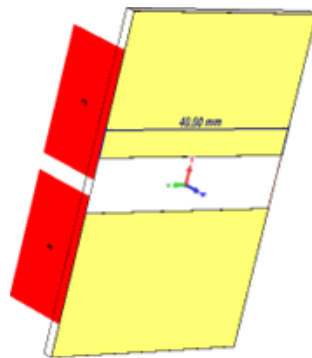


Fig. 2. Harmonic suppression layout

3. RESULTS AND DISCUSSION

This section will include all the findings to examine how well the Wilkinson Power Divider with harmonic suppression performs. It will then provide a deeper understanding by analysing theoretical and simulation results based on the behaviour of power dividers.

3.1 Return Loss Before and After Adding a Suppressing Element

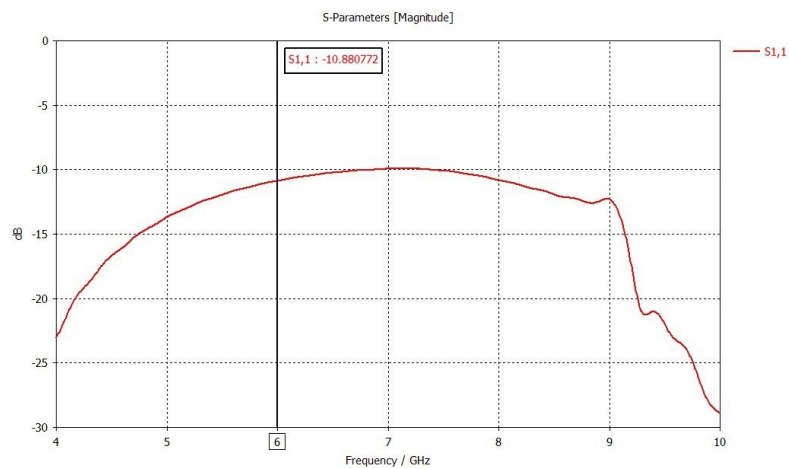


Fig. 3. S11 result without suppressing element

The return loss (S11) of this design without suppressing element is displayed on an S—S-parameter plot throughout the frequency range of 4 GHz to 10 GHz, with an emphasis on 6 GHz, where S11 is around -10.88 dB based on Figure 3.

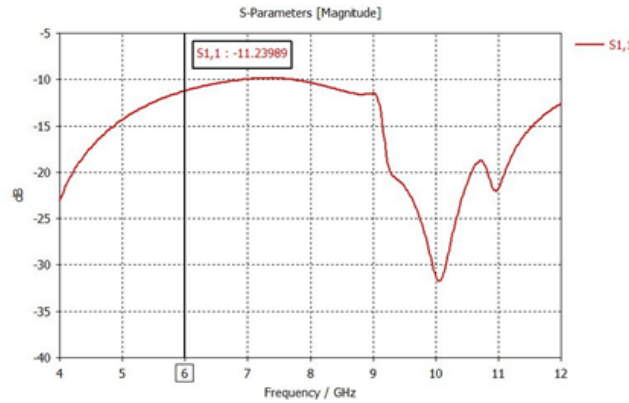


Fig. 4. S11 results in suppressing element

Meanwhile, Figure 4 shows that the return loss at 6 GHz is -11.24 dB which means the component transmits 92% of the incident power and reflects around 8% of it back to the source. In addition, the figure displays different return losses at different frequencies. Near 10 GHz, improved impedance matching is shown, as seen by the lower S11 value. As can be viewed from both figures, the return loss values improved from -10.88 dB to -11.24 dB. This means that the amount of signal being reflected to the input port is reduced.

3.2 Impedance Matching Before and After Adding a Suppressing Element

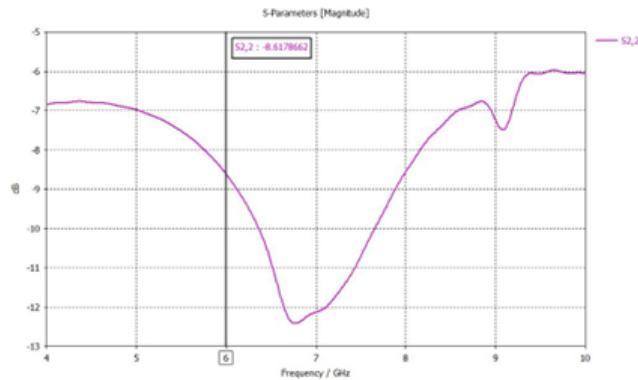


Fig. 5. S22 result without suppressing element

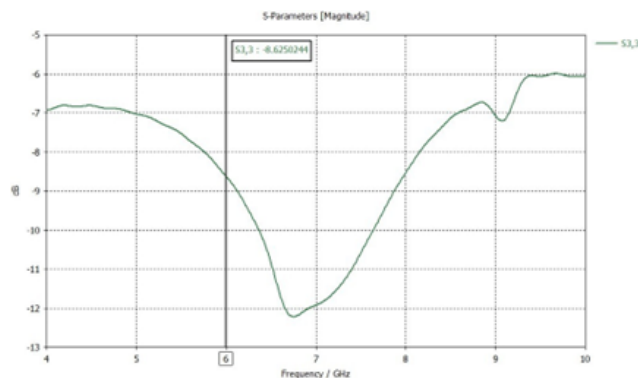


Fig. 6. S33 result without suppressing element

The S22 and S33 parameters measure impedance matching, which is crucial for reducing signal reflections at the output ports of a Wilkinson power divider. S22 and S33 are the metrics used to quantify the reflection at Port 2 and Port 3,

respectively. Figures 5 and 6 illustrate that the S_{22} values without suppressing elements are around -8.6 dB for both figures.

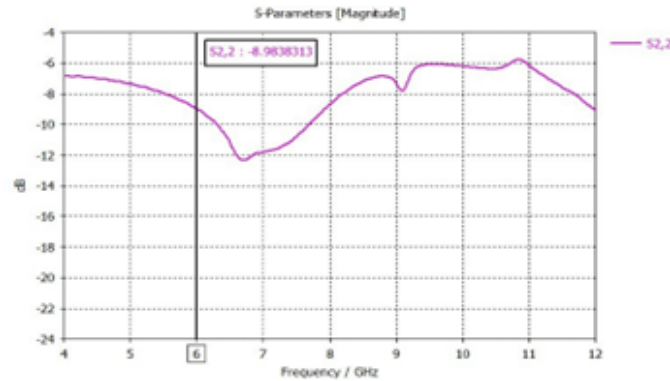


Fig. 7. 7 $S_{2,2}$ result with suppressing element

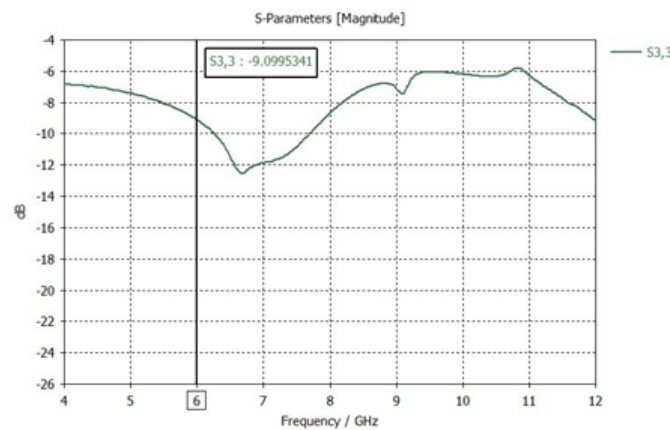


Fig. 8 $S_{3,3}$ result with the suppressing element

However, with the suppressing element, the S-parameters plotted above show suboptimal impedance matching at the output ports, port 2 and port 3. In the S_{22} and S_{33} graphs above, they represent an approximate value of -9 dB. The value of -9 dB for S_{22} and S_{33} indicates that the system is functioning, but it is far from optimal and should be improved for better performance and efficiency. Nevertheless, it appears that the addition of the suppressing element improves the impedance matching across the entire frequency range, as shown by the lower values for S_{22} and S_{33} , which means that most of the signal is passed through the ports with little reflection.

3.3 Insertion Loss Before and After Adding a Suppressing Element

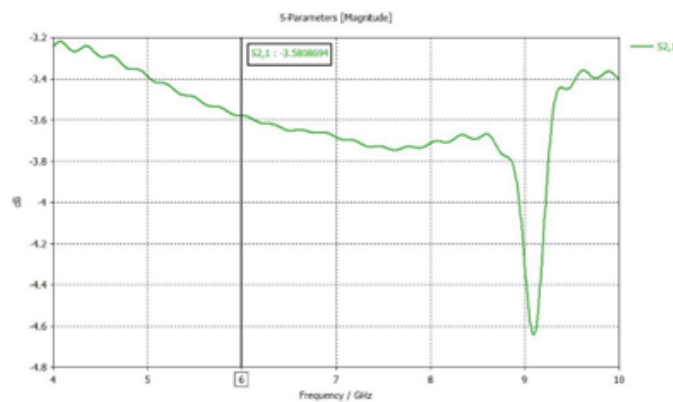


Fig. 9. $S_{2,1}$ result without suppressing element

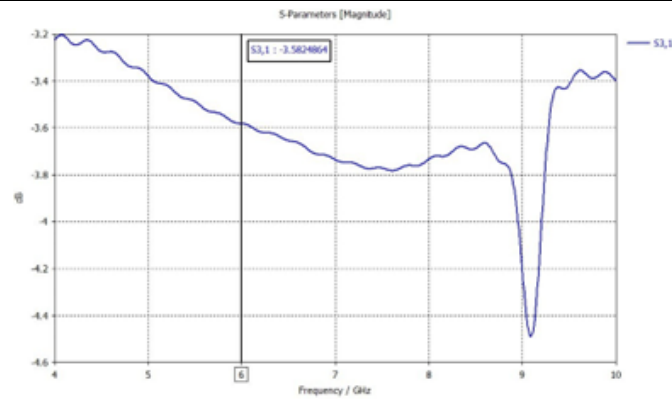


Fig. 10. S31 result without suppressing element

The attenuation or loss of a signal experienced when passing via the Wilkinson Power Divider from Port 1 to Port 2 (S21) or Port 3 (S31) is illustrated in Figures 9 and 10, respectively. For a Wilkinson Power Divider to show uniform power distribution to every output port, its insertion loss should ideally be -3 dB. The insertion loss based on the above figures without harmonic suppression is around -3.58 dB at Ports 2 and 3.

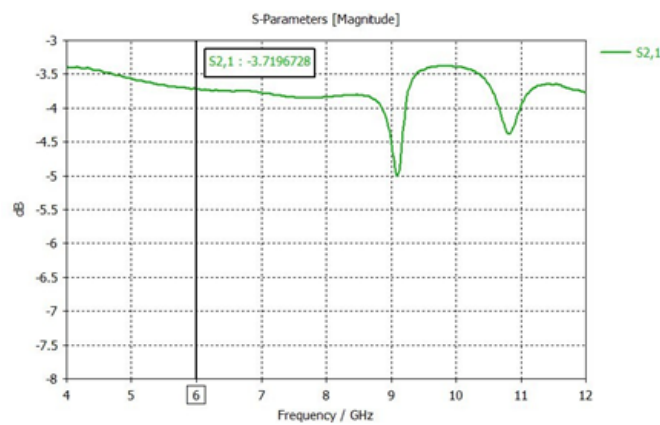


Fig. 11. S21 results with suppressing element

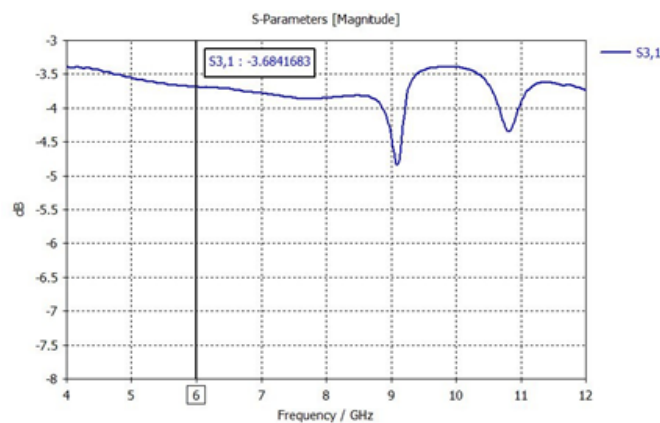


Fig. 12. S31 results with suppressing element

As in Figures 11 and 12, this design with harmonic suppression gained its insertion loss at port 2 and port 3 to approximately -3.7 dB, respectively. The value is still acceptable, as it is near -3 dB. The goal is to minimise insertion loss to guarantee effective signal transmission. Lower insertion loss levels indicate more signal deterioration and improved performance.

3.1. Mutual Coupling Before and After Adding a Suppressing Element

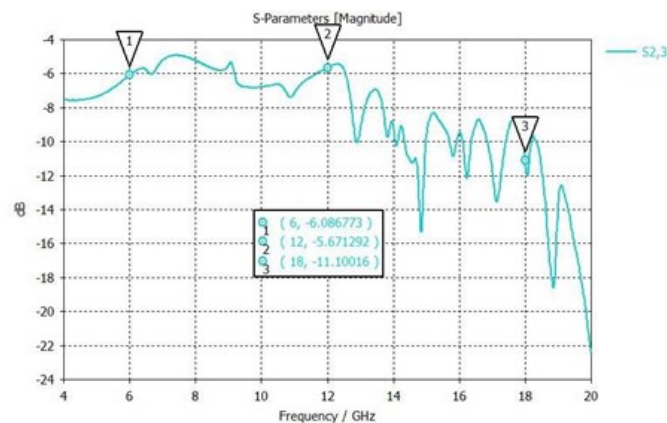


Fig. 13. S23 result without suppressing element

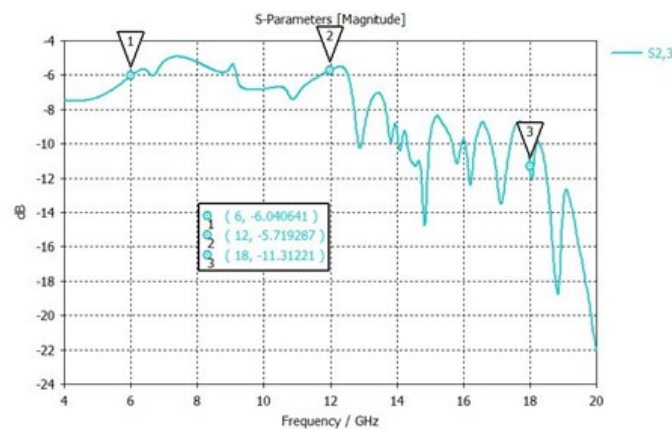


Fig. 14. S23 results with suppressing element

Figure 13 and Figure 14 depict the S23 results, which is the mutual coupling between output port 2 and output port 3. In this segment, three harmonics need to be observed in order to see the value of mutual coupling before and after the suppression element is added. Between Figure 4.5.1 and Figure 4.5.2, at 6 GHz, the harmonics are not sufficiently reduced from -6.08 dB to -6.04 dB. However, in the 2nd harmonic at 12 GHz, the value of mutual coupling is efficiently reduced from -5.67 dB to -5.71 dB. Also, in the 3rd harmonic at 18 GHz, the mutual coupling is sufficiently reduced from -11.10 dB to -11.31 dB. Hence, it proved that the signals at one port do not interfere with signals at the other port. However, due to flaws in the componentry or layout, there may still be some degree of mutual interaction in actual implementations.

4. CONCLUSION

This paper presents a modified WPD with good isolation and harmonic suppression structure. The proposed design requires cutting some part of the copper slot, which is one method used to suppress the harmonics. According to the results obtained, the WPD has a good performance at 6 GHz, which is suitable for mobile applications.

REFERENCES

- [1] "Choosing the Right Power Divider for Your RF System," www.rfone.cn. <https://www.rfone.cn/blog-detail/choosing-the-right-power-divider-for-your-rf-system> (accessed Dec. 15, 2023).

-
- [2] L. J. Berens, "Design, Analysis, and Construction of an Equal Split Wilkinson Power Divider," Jan. 2012.
- [3] H. Elftouh, M. E. Bakkali, N. T. Amar, A. Zakriti, A. Mchbal, and A. Dkiouak, "The Unequal Wilkinson Power Divider 2:1 for WLAN Application," *Procedia Manufacturing*, vol. 46, pp. 777–781, 2020, doi: <https://doi.org/10.1016/j.promfg.2020.04.004>.
- [4] Gholamhosein Moloudian, A. Lalbakhsh, and S. Bahrami, "A Harmonic-Free Wilkinson Power Divider Using Lowpass Resonators," 2022 16th European Conference on Antennas and Propagation (EuCAP), Mar. 2022, doi: <https://doi.org/10.23919/eucap53622.2022.9769082>.
- [5] A. Mandal, Tamasi Moyra, and P. Paul, "Compact Low-pass Filtering-response Wilkinson Power with Wide Harmonic Suppression," Mar. 2023, doi: <https://doi.org/10.1109/ccwc57344.2023.10099359>.
- [6] S. Abbas, M. Maqsood, N. Shoaib, Muhammad Qasim Mehmood, M. Zubair, and Y. Massoud, "A Wideband RF Power Divider with Ultra-Wide Harmonics Suppression," *IEEE Journal of microwaves*, vol. 3, no. 4, pp. 1248–1257, Oct. 2023, doi: <https://doi.org/10.1109/jmw.2023.3307654>.
- [7] Z. Wang, N. Zhang, X. Wang, Z. Ma, and C.-P. Chen, "Miniaturized Horst-type Wilkinson Power Divider with Harmonic Suppression," Dec. 2020, doi: <https://doi.org/10.1109/apmc47863.2020.9331394>.
- [8] Gholamhosein Moloudian, S. Soltani, S. Bahrami, J. L. Buckley, B. O'Flynn, and A. Lalbakhsh, "Design and fabrication of a Wilkinson power divider with harmonic suppression for LTE and GSM applications," vol. 13, no. 1, Mar. 2023, doi: <https://doi.org/10.1038/s41598-023-31019-7>.
- [9] Ceyhun Karpuz, Mehmet Çakır, Ali Kürşad Görür, and Adnan Görür, "Design of N-Way Wilkinson Power Dividers with New Input/Output Arrangements for Power Halving Operations," May 2023, doi: <https://doi.org/10.20944/preprints202305.0773.v1>.
- [10] Y. Ding, J. Wan, Y. Yan, and X. Liang, "A Novel Compact, Wideband Four-Way Wilkinson Power Divider with an Improved Isolation Topology," *IEEE Microwave and Wireless Technology Letters*, vol. 33, no. 8, pp. 1119–1122, Aug. 2023, doi: <https://doi.org/10.1109/lmwt.2023.3279898>.
- [11] M. Kumar, N. Islam, G. Sen, Susanta Kumar Parui, and S. Das, "Design of Compact Wilkinson Power Divider with Harmonic Suppression for GSM Application," Dec. 2017, doi: <https://doi.org/10.1109/aemc.2017.8325635>.
- [12] Maizun Jamil & Nurul Najwa Md Yusof, "A Review of Wilkinson Power Divider as A Splitter/Combiner Based on Method, Design and Technology," December 2020.
-